

Microscale Parallel Synthesis of Acylated Aminotriazoles Enabling the Development of Factor XIIa and Thrombin Inhibitors

Simon Platte,^[a] Marvin Korff,^[a] Lukas Imberg,^[a] Ilker Balicoglu,^[a] Catharina Erbacher,^[b] Jonas M. Will,^[b] Constantin G. Daniliuc,^[c] Uwe Karst,^[b] and Dmitrii V. Kalinin*^[a]

Dedicated to the memory of Professor B. Ya. Syropyatov, our mentor, colleague, and blood coagulation expert

Herein we report a microscale parallel synthetic approach allowing for rapid access to libraries of N-acylated aminotriazoles and screening of their inhibitory activity against factor XIIa (FXIIa) and thrombin, which are targets for antithrombotic drugs. This approach, in combination with post-screening structure optimization, yielded a potent 7 nM inhibitor of FXIIa and a 25 nM thrombin inhibitor; both compounds showed no inhibition of the other tested serine proteases. Selected N-

acylated aminotriazoles exhibited anticoagulant properties *in vitro* influencing the intrinsic blood coagulation pathway, but not extrinsic coagulation. Mechanistic studies of FXIIa inhibition suggested that synthesized N-acylated aminotriazoles are covalent inhibitors of FXIIa. These synthesized compounds may serve as a promising starting point for the development of novel antithrombotic drugs.

Introduction

Thrombosis is a life-threatening pathology characterized by a thrombus (blood clot) formation inside a vein or an artery. The formed thrombus may completely or partially block the blood supply to major organs causing their ischemia, dysfunction, and failure. Thus, acute arterial and venous thromboses are associated with myocardial infarction, ischemic stroke, and pulmonary embolism, which are the main reason of death in developed countries.^[1]

Anticoagulant drugs are commonly used for the prevention of thrombosis and associated cardiovascular pathologies. Among anticoagulants, injectable heparins are routinely used in clinical settings, whereas vitamin K antagonists and direct thrombin and FXa inhibitors are orally available and are among the most frequently prescribed drugs.^[2] Several examples of

approved and developmental anticoagulants are shown in Figure 1.^[3] Despite their efficacy, all available anticoagulants exhibit side effects, of which the risk of causing major bleeding is universal and the most dangerous.^[4] For example, individuals receiving oral anticoagulants have a 7–10 times higher chance to develop intracranial bleeding, which in about 50% of cases is lethal or may result in severe disability.^[5] Therefore, novel anticoagulants causing no bleeding complications are highly desired.

The ideal anticoagulant should prevent pathological thrombus formation without affecting the physiological hemostatic

- [a] S. Platte, M. Korff, L. Imberg, I. Balicoglu, Dr. D. V. Kalinin
Institute of Pharmaceutical and Medicinal Chemistry
University of Münster
Corrensstr. 48, 48149 Münster (Germany)
E-mail: dmitrii.kalinin@uni-muenster.de
- [b] C. Erbacher, Dr. J. M. Will, Prof. U. Karst
Institute of Inorganic and Analytical Chemistry
University of Münster
Corrensstr. 30, 48149 Münster (Germany)
- [c] Dr. C. G. Daniliuc
Institute for Organic Chemistry
University of Münster
Corrensstr. 40, 48149 Münster (Germany)

Supporting information for this article is available on the WWW under <https://doi.org/10.1002/cmdc.202100431>This article belongs to the Early-Career Special Collection, "EuroMedChem Talents".

© 2021 The Authors. ChemMedChem published by Wiley-VCH GmbH. This is an open access article under the terms of the Creative Commons Attribution Non-Commercial License, which permits use, distribution and reproduction in any medium, provided the original work is properly cited and is not used for commercial purposes.

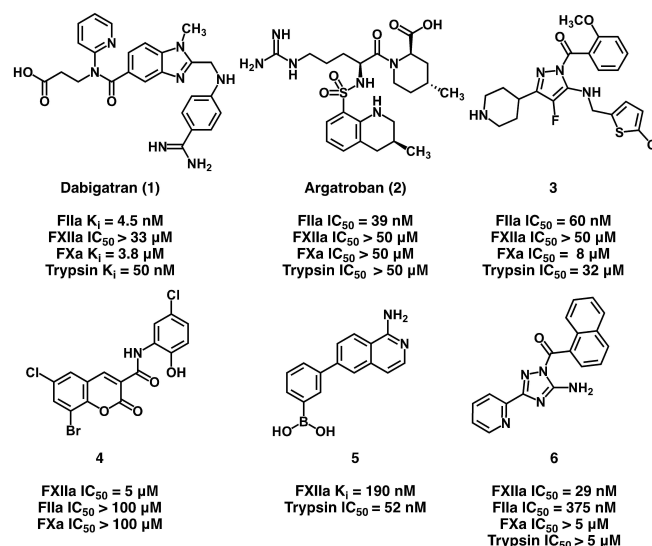


Figure 1. Exemplary thrombin inhibitors (1-3) and FXIIa inhibitors (4-6). Provided are the K_i values or the IC_{50} values toward thrombin, FXIIa, and other physiologically relevant serine proteases.^[3]

function. To develop such a drug, alternative targets in the blood coagulation system should be addressed. In this respect, coagulation factor XIIa (FXIIa), also known as the Hageman factor, has recently emerged as a new target for safe anticoagulation.^[6] FXIIa is a serine protease (Figure 2) initiating the intrinsic blood coagulation pathway and the kallikrein/kinin system. Consequently, the proteolytic activity of FXIIa is associated with thrombosis and inflammation. However, the deficiency of this enzyme is practically asymptomatic.^[7] FXII-deficient animals and those treated with FXIIa inhibitors are protected from thrombosis and also show no tendency to injury-induced bleeding.^[6a,7] These facts characterize FXIIa as a promising target for thrombosis prevention.

Apart from FXIIa, thrombin (Figure 2), a classical target for anticoagulation therapy, can potentially be a safe target if addressed with a specific inhibitor. For instance, it has been shown that direct thrombin inhibitor VE-1902 (no exact structure is disclosed by the authors) modulate blood coagulation preventing thrombosis in animals with only a little effect on bleeding time due to its reversible covalent mechanism of action.^[3c,10] The lower bleeding risk for VE-1902 was linked to its reduced ability to inhibit thrombin-mediated platelet activation.^[10] VE-1902 was attributed to a new class of precision oral anticoagulants (PROACs) and it is currently in phase 1 clinical trial.

Many examples of small molecular direct thrombin inhibitors are known, including the marketed oral drug dabigatran and injectable argatroban (Figure 1).^[3a,b] None of them, however, is similar to VE-1902 in terms of the covalent reversible mechanism of thrombin inhibition and the related reduced tendency to cause bleeding. Significantly fewer inhibitors of FXIIa are known and none of them is yet approved for clinical application.^[6a] Moreover, FXIIa inhibitors mainly belong to peptides, proteins, and monoclonal antibodies. Their small molecular counterparts, which could potentially be used as highly desired oral anticoagulants, are represented by only a few examples (4–6, Figure 1).^[6,11]



Dr. Dmitrii V. Kalinin, born in 1986, started his research career in Russia, where he received his degree in pharmacy in 2009. In 2012, Dmitrii joined the group of Prof. A. Dolzhenko at the Curtin University of Technology (Perth, Australia) where he worked on the synthesis of heterocyclic compounds. In 2013, Dmitrii joined the international "Cells in Motion" graduate school at the University of Münster (Germany), where in 2017 under the supervision of Prof. R. Holl and Prof. B. Wünsch he obtained his PhD degree. In 2018, after one year of postdoctoral studies at the University of Southern Denmark (Prof. T. Ulven's group), Dmitrii returned to the University of Münster to start his independent research group. His research activities are in the field of Medicinal Chemistry and Drug Design. He focuses on the development of novel antithrombotic drugs.

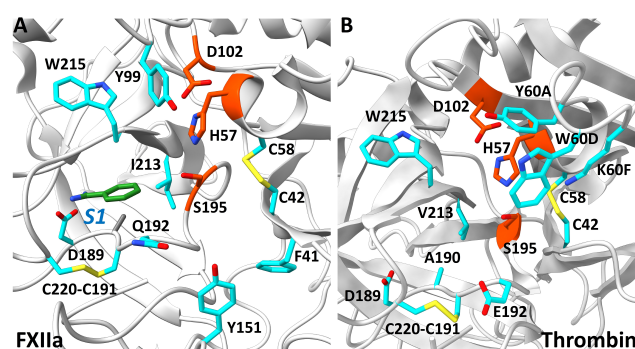


Figure 2. The active site of FXIIa (A) and thrombin (B), PDB: 6B74^[3e] and 1A4W^[8] respectively. The residues are depicted as cyan stick models; the catalytic residues (His57, Asp102, Ser195, chymotrypsin numbering system) are shown in orange. For XIIa, the ligand (benzamidine) residing in the S1 selectivity pocket is shown in green. Molecular graphics were prepared with UCSF ChimeraX.^[9]

Our recent studies and studies from other groups suggest that N-acylated aminotriazoles and aminopyrazoles can act as covalent reversible inhibitors of FXIIa and thrombin exhibiting anticoagulant properties (e.g., compounds **3** and **6**, Figure 1).^[3c,f,12] At that, structural variations on their N-acyl moiety as well as on their azole core allow to access inhibitors with different physicochemical properties and unique serine protease inhibitory profiles.^[3f] However, the development of a potent and selective inhibitor requires the generation of big libraries of N-acylated azoles and their subsequent screening against multiple serine proteases. Using conventional methods, this is a challenging task requiring significant amounts of consumables and multiple synthetic and purification efforts. To overcome these obstacles and intensify the development of new FXIIa and thrombin inhibitors, we developed a microscale parallel synthetic approach enabling us to fast access libraries of N-acylated aminotriazoles and screen their inhibitory activity against FXIIa and thrombin.

Results and Discussion

Method Design

A new method allowing for the efficient search for novel FXIIa and thrombin inhibitors should satisfy several criteria. Firstly, it should allow fast synthesis of N-acylated aminotriazoles in a parallel fashion. Secondly, it should utilize small quantities of inexpensive consumables, including reactants, solvents, and glassware. Also, the method should avoid or minimize the purification steps. Lastly, it should allow high- or medium-throughput screening of synthesized compounds in biological assays.

The prospective inhibitors are composed of two parts (e.g., inhibitors **3** and **6**, Figure 1) namely the aminoazole fragment (FR1) and the acyl fragment (FR2), of which FR1 requires synthetic preparation, whereas FR2 is commercially available.

Having both fragments in hand, they can be assembled in a microscale coupling reaction in a 96-well plate. Using this approach, structurally diverse FR1 and FR2 can be linked to each other in a combinatorial fashion in parallel (Figure 3). To avoid the time- and material-consuming purification steps, the

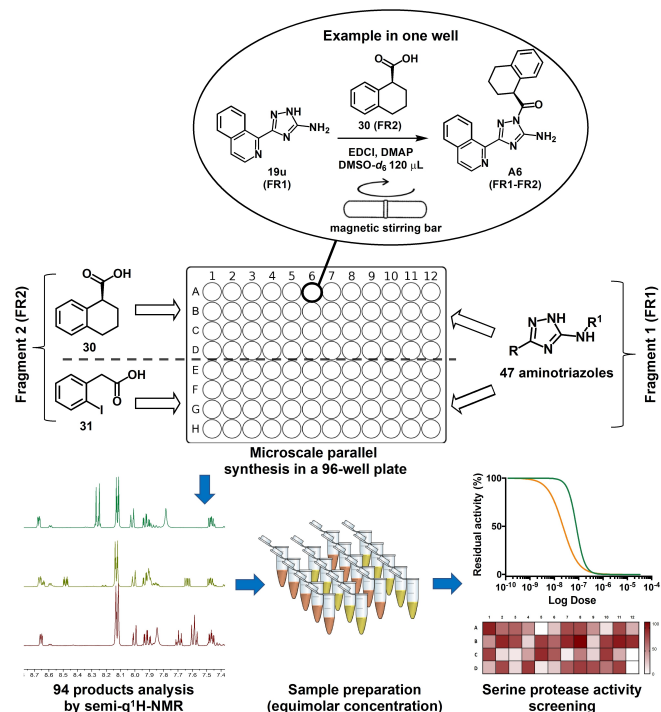


Figure 3. Schematic representation of the microscale parallel synthetic approach combined with medium-throughput screening (MTS) toward FXIIa and thrombin inhibitors. The aminotriazole fragments and the acyl fragments are denoted as FR1 and FR2, respectively.

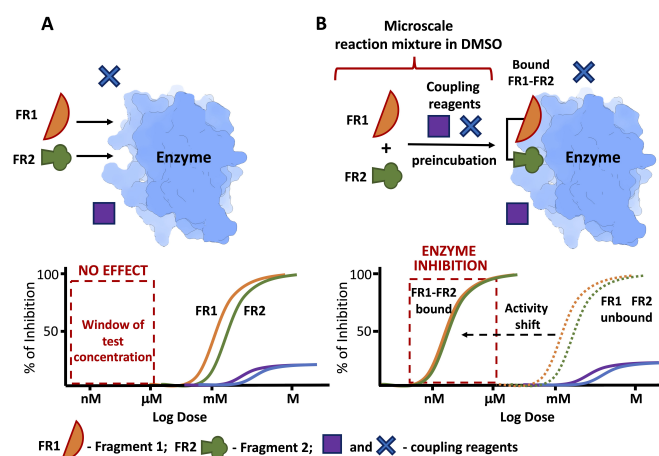


Figure 4. The principle of the inhibitory activity testing of microscale-reactions against FXIIa and thrombin. The unbound fragments FR1 and FR2 and the coupling reagents (X- and square-shaped figures) are low active inhibitors of the enzymes and do not interfere with the assay at low concentrations (A). When FR1 and FR2 are bound together, a significant shift in inhibitory activity is observed (B). When the reaction mixtures are tested at nM or low μ M concentrations, only the inhibitory effect of the bound fragments FR1-FR2 is detected enabling screening.

microscale reaction mixtures, containing bound fragments, should be directly (without isolation) screened for the inhibitory activity against selected serine proteases. To make sure that each final product (FR1-FR2 bound) is screened for the activity in an equimolar concentration, the products should be quantified before being screened (Figure 3). Based on the results of the screening, the hits should be selected and synthesized in a conventional reaction scale and tested for their biological activity as pure individual compounds.

The direct screening of crude microscale-reaction mixtures was proposed as a feasible approach based on the principle illustrated in Figure 4. The unbound fragments FR1 and FR2 (shown as orange and green figures) and the coupling reagents (shown as X- and square-shaped figures) are low active or inactive inhibitors of FXIIa and thrombin and do not interfere with the assay at low concentrations (Figure 4, A). We previously showed that the unbound fragments FR1 and FR2 cannot efficiently inhibit the enzymes as only connected fragments (FR1-FR2) are capable of covalent interaction with the enzymes' catalytic Ser195 (also see the "Mechanism of Inhibition" section).^[3f] Accordingly, when FR1 and FR2 are bound to each other forming N-acylated aminotriazole, a significant shift in inhibitory activity is observed (toward lower doses, Figure 4, B). Therefore, when the reaction mixtures are tested at nM or low μ M concentrations (of the reaction product), only the inhibitory effect of the bound fragments FR1-FR2 is detected enabling screening. This excludes the chance of false-positive results caused by unreacted fragments.

Method Development

At first, we developed a method allowing microscale parallel synthesis of N-acylated aminotriazoles in 96-well plates. For this, we selected 1*H*-1,2,4-triazol-5-amine **7**, a non-acylated scaffold of inhibitor **6** (Figure 1), as a model aminotriazole fragment (FR1) and five structurally different carboxylic acids (**8**–**12**) as acyl fragments (FR2). Particularly, benzoic acid (**8**), nicotinic acid (**9**), 4-methoxybenzoic acid (**10**), tetrahydro-2*H*-pyran-4-carboxylic acid (**11**), and *N*-benzoyl-L-proline (**12**) were selected. To construct the N-acylated aminotriazoles (FR1-FR2), the azole's annular nitrogen atom requires to react with the carboxylic acids. For carboxylic acids being poor electrophiles, the reaction with an amine does not happen spontaneously. Currently, however, many robust methods are described for the amide bond formation, e.g., the use of activated carboxylic acid derivatives like acid chlorides and anhydrides, or the use of transition metal catalysts, microwave irradiation, as well as peptide coupling reagents.^[13]

For their high reactivity, acid chlorides and anhydrides are not suitable for the microscale reactions coupled with the direct biological activity screening as they could interact with the enzymes thereby interfering with the assay. Besides, many acid chlorides exhibit limited shelf stability and require synthesis under water-free conditions. Transition metal catalysts also often require anhydrous and oxygen-free reaction conditions and prior to the analytics and the inhibition assays, the metal

must be removed from the solution. In contrast, for the reason of reaction performance simplicity and availability of a number of bench-stable carboxylic acids and coupling reagents, the peptide coupling was considered as the most suitable method for our microscale experiments.

The method development, as well as the subsequent screening, required a robust way of the reaction product quantification. Three quantitation methods were tested, namely HPLC-UV, HPLC-MS, and semi-quantitative $^1\text{H-NMR}$ (semi-q $^1\text{H-NMR}$). Of them, HPLC-UV and HPLC-MS were found to be less practical due to relatively long spectra processing time, difficulties with analyzing complex reaction mixtures, and the requirement of external standard for proper reaction product quantification. In contrast, the semi-q $^1\text{H-NMR}$ method allowed fast reaction product quantification irrespective of the ionization and UV-absorption properties of starting materials and products. The semi-q $^1\text{H-NMR}$ principle used for the analysis of

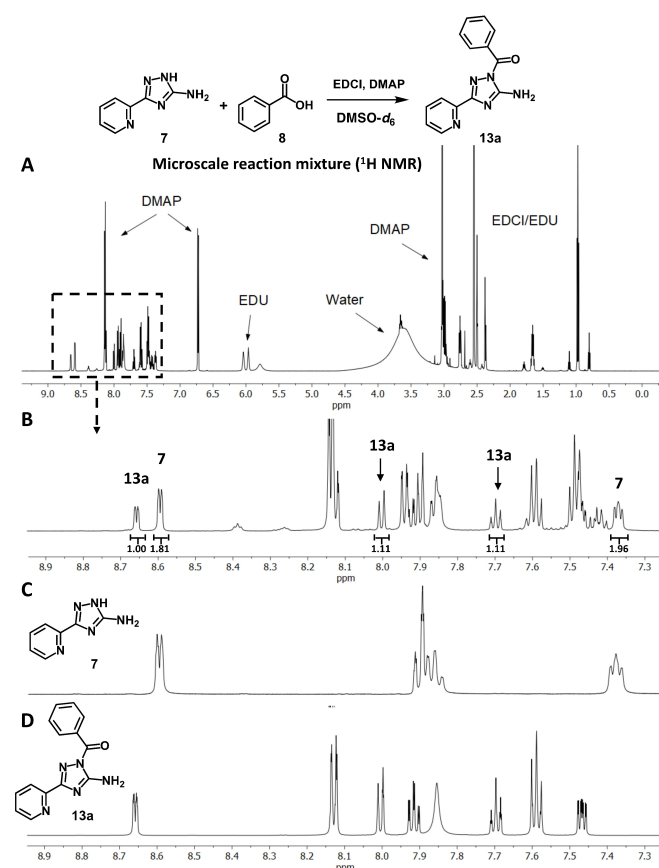


Figure 5. Exemplary $^1\text{H-NMR}$ spectrum of the microscale reaction mixture in $\text{DMSO-}d_6$, overall view (A) and a close-up view at 7.3–8.9 ppm (B) stacked against spectra of the starting material aminotriazole **7** (C) and the reaction product **13a** (D) in $\text{DMSO-}d_6$. Spectrum B shows the integration of isolated characteristic signals of the starting material (**7**) and the product (**13a**) used for the reaction conversion calculation. The use of the pyridyl moiety's 6'-H signal is the most convenient for the reaction conversion calculation as it experiences a low-field shift (from 8.59 ppm to 8.66 ppm) upon successful coupling reaction irrespective of the acyl moiety structure. The reaction conversion rate is calculated to be 36% (**13a**, entry 3, Table 1). The calculation details are shown in the Experimental Section.

the microscale reaction mixtures is shown in Figure 5, Figure 6, and the Experimental Section.

The method development was performed in a 96-well plate reacting aminotriazole **7** (3 mg, 18.6 μmol , each well) with the carboxylic acids **8–12** (1 equiv. each) in $\text{DMSO-}d_6$ (120 μL) varying the amide coupling reaction conditions to maximize the average yield of N-acylated aminotriazoles **13a–e** (Table 1). We attempted the first three typical amide coupling conditions (entries 1–3, Table 1), of which COMU/DIPEA and HATU/DIPEA resulted in no desired products formation. In contrast, the combination of EDCI/DMAP produced N-acylated aminotriazoles with an average conversion of 38% in 16 h at 50 $^\circ\text{C}$ (entry 3). The average conversion was increased to 62%, when the reaction temperature was reduced from 50 $^\circ\text{C}$ to room temperature (entry 4). The reaction time prolongation to 92 h, however, resulted in the average conversion decrease to 32% (entry 5). Entries 3–5 indicate that upon temperature elevation or the reaction time prolongation, lower yields are observed, which is associated with the degradation of the acylated product rather than with the low reactivity of the reacting species (see the DMAP-promoted decomposition, Supporting Information, Table S1).

The increase of EDCI/DMAP equivalents (to 1.5 each), as well as the addition of micromagnetic stirring bars into each well of

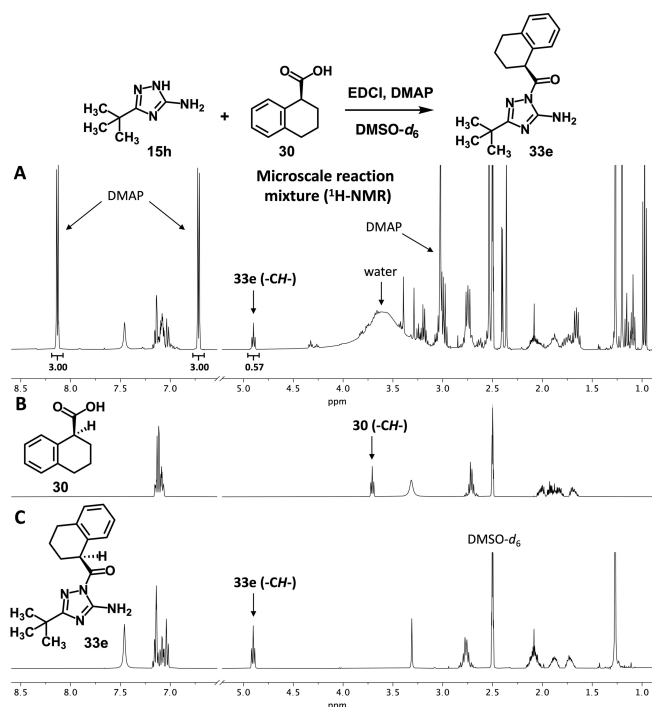


Figure 6. A fragment of $^1\text{H-NMR}$ spectrum of an exemplary microscale reaction mixture (A) stacked against spectra of the starting material carboxylic acid **30** (B) and the reaction product **33e** (C) in $\text{DMSO-}d_6$. The characteristic proton signal of the methine group of **30** (B) experiences a low-field shift upon successful coupling reaction (product **33e** formation (C)) irrespective of the aminotriazole structure and, therefore, was used for the reaction conversion calculation. DMAP, which concentration remains unchanged, was used as an internal standard. The reaction conversion rate was calculated to be 57%. The calculation details are shown in the Experimental Section.

Table 1. Optimization of the parallel microscale amide coupling reactions performed in a 96-well plate.^[a]

Entry	Coupling reagent/base (equiv./equiv.)	Stirring ^[c]	Temperature [°C]	Reaction time [h]	Reaction conversion [%] ^[b]	Structure of acyl fragment (FR2)					Average conversion [%]
						13 a	13 b	13 c	13 d	13 e	
1	COMU/DIPEA (1.1/1.1)	–	50	16	–	–	–	–	–	–	–
2	HATU/DIPEA (1.1/1.1)	–	50	16	–	–	–	–	–	–	–
3	EDCI/DMAP (1.1/1.1)	–	50	16	36	6	60	54	34	38	
4	EDCI/DMAP (1.1/1.1)	–	r.t.	16	63	39	79	77	54	62	
5	EDCI/DMAP (1.1/1.1)	–	r.t.	92	31	1	73	23	31	32	
6	EDCI/DMAP (1.5/1.5)	–	r.t.	16	79	58	92	94	67	78	
7	EDCI/DMAP (1.1/1.1)	+	r.t.	16	73	48	84	88	58	70	
8	EDCI/DMAP (1.5/1.5)	+	r.t.	16	85	71	91	92	56	79	
9 ^[d]	EDCI/DMAP (1.5/1.5)	+	r.t.	16	80	46	93	90	61	74	
10	EDCI (1.5)	+	r.t.	16	12	30	9	14	29	19	
11	EDCI/HOBt (1.5/1.5)	+	r.t.	16	6	2	34	64	82	38	
12	EDCI/DIPEA (1.5/3.0)	+	r.t.	16	25	27	21	11	10	19	
13	DCC/DMAP (1.5/1.5)	+	r.t.	16	46	32	39	60	31	42	
14 ^[e]	EDCI/DMAP (1.5/1.5)	+	r.t.	16	88	74	93	96	55	81	
15	EDCI/DMAP (1.5/1.5)	+	r.t.	3	87	72	82	85	53	76	

^[a] Reaction conditions: in one well of 96-well plate, in DMSO-*d*₆ (120 μL), **7** (3 mg, 18.6 μmol) reacted with a carboxylic acid (1 equiv.) in the presence of indicated coupling reagent and base at the indicated temperature and reaction time. ^[b] As measured by semi-^qH-NMR. ^[c] Micro magnetic stirring bars implemented into each well of the well plate were used; ^[d] 1.1 equiv. of carboxylic acid was used; ^[e] The reaction was performed under an N₂ atmosphere

the well plate, were beneficial, further increasing the reaction average conversion up to 79% (entries 6–8). Neither the excess of carboxylic acids (entry 9) nor the base (DMAP) removal or its substitution (entries 10–12) improved the reactions' yield. Also, EDCI replacement with a similar coupling reagent DCC had no positive effect on the yield of the microscale reactions (entry 13). Performing reactions under a dry inert atmosphere (the well-plate was placed into a desiccator with phosphorus pentoxide under N₂), resulted only in a slight improvement (81%, entry 14) when compared to the reaction under ambient atmosphere (79%, entry 8). Lastly, the experiments with shortened reaction time (3 h, entry 15) have been performed leading to a slightly decreased average conversion (76%) compared to 16 h reaction time (79%, entry 8). An extended table with additional reaction conditions is shown in the Supporting Information (Table S2).

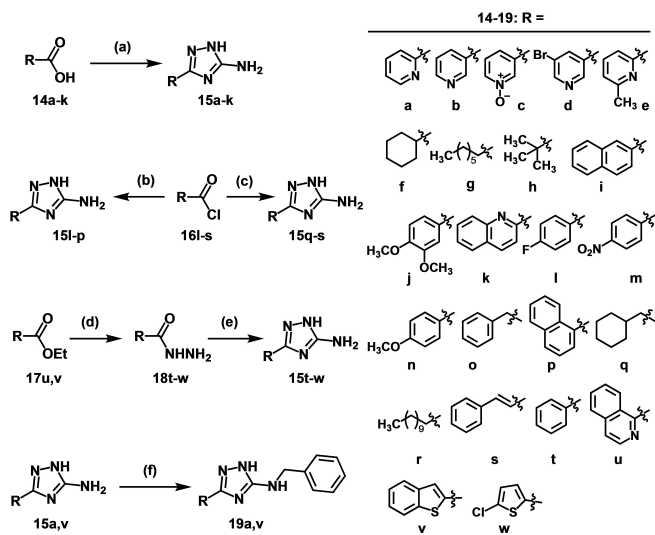
Because of the high effort for moisture-free reaction conditions, compared to the low benefit (cf. entry 8 and 14), as well as the low negative impact of shortened reaction time, the reaction conditions of entry 15 have been selected for the actual microscale parallel synthesis. Utilizing optimized reaction conditions, microscale parallel synthesis of 95 N-acylated aminotriazoles based on 1H-1,2,4-triazol-5-amine **7** (FR1) and 95 structurally diverse carboxylic acids (FR2) was performed. The resultant library of compounds was screened against FXIIa and thrombin revealing potent dual and selective inhibitors of FXIIa and/or thrombin. The results of this screening have been disclosed by us earlier and will not be repeated here.^[3f] The screening was limited only to the variations on the inhibitors'

acyl fragment (FR2), leaving the aminotriazole core (FR1) unchanged and therefore unexplored. Now, knowing the structures of the most promising acyl moieties, we will retain them unchanged while varying the other structural features of the inhibitor, particularly its aminotriazole core.

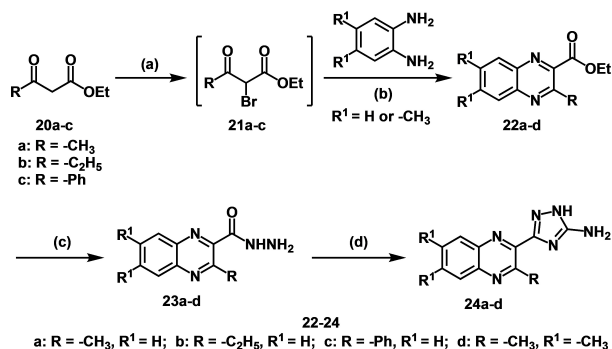
Conventional Synthesis of 1H-1,2,4-triazol-5-amines (FR1)

To generate a library of structurally diverse 1H-1,2,4-triazol-5-amines (FR1) exhibiting non-acylated triazole *N*-atom, syntheses shown in Schemes 1–3 were performed. The rationale behind the selection of substituents in the 3-position of the triazole core was based on the idea that the triazole core should be extended toward enzymes' S1' and S3-S4 substrate binding sites, which were previously not addressed by this class of compounds, to improve the inhibitors' binding affinity toward thrombin and/or FXIIa.

Aminotriazoles **15a–k** were synthesized in a fusion reaction between aminoguanidine hydrochloride and carboxylic acids **14a–k** at 200 °C (Scheme 1). The reaction proceeds via intermediate amidoguanidines, which subsequently, without isolation undergo a cyclocondensation reaction affording desired products **15a–k**.^[3f] Similarly, aminotriazoles **15l–s** were accessed reacting corresponding acid chlorides with aminoguanidine salts under basic conditions (Scheme 1). Other aminotriazoles **15t–w** were obtained via the treatment of hydrazides **18t–w** with 5-methylisothiuronium sulfate, which also produces intermediate amidoguanidines followed by their

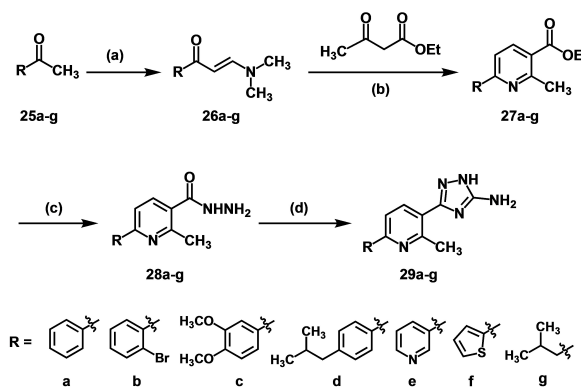


Scheme 1. Synthesis of *1H*-1,2,4-triazol-5-amines **15a-w** and **19a,v**: (a) aminoguanidine hydrochloride, neat, 200 °C, 4 h, **15a** 70%, **15b** 74%, **15c** 45%, **15d** 72%, **15e** 42%, **15f** 32%, **15g** 30%, **15h** 28%, **15i** 29%, **15j** 12%, **15k** 79%; (b) 1. aminoguanidine hydrochloride, KOH, H₂O/THF, 0 °C, 1 h; 2. NaHCO₃, H₂O/THF, reflux, 4 h, **15l** 58%, **15m** 83%, **15n** 34%, **15o** 31%, **15p** 12%; (c) 1. aminoguanidine bicarbonate, pyridine, r.t., 24 h; 2. NaHCO₃, H₂O/THF, reflux, 4 h, **15q** 10%, **15r** 31%, **15s** 28%; (d) NH₂NH₂·H₂O, EtOH, reflux, 1.5–2 h, **18u** 75%, **18v** 87%; (e) 1. *S*-methylisothiuronium sulfate, EtOH/H₂O, reflux, 16–72 h, 2. KOH (40%), reflux 2–4 h, **15t** 57%, **15u** 17%, **15v** 24%, **15w** 32%; (f) 1. benzaldehyde, THF/toluene, reflux, 18 h; 2. NaBH(OAc)₃, DCM, r.t., 18 h, **19a** 26%, **19v** 23%.



Scheme 2. (a) NBS, H₂O, 70 °C, 1–3 h; (b) H₂O, 70 °C, 3–4 h, **22a** 23%, **22b** 43%, **22c** 31%, **22d** 21%; (c) NH₂NH₂·H₂O, EtOH, reflux, 2–3 h, **23a** 74%, **23b** 65%, **23c** 86%, **23d** 74%; (d) 1. *S*-methylisothiuronium sulfate, EtOH/H₂O, reflux, 48–72 h, 2. KOH, EtOH/H₂O, reflux 3–6 h, **24a** 32%, **24b** 28%, **24c** 33%, **24d** 41%.

cyclization (Scheme 1). The necessity of having all three synthetic strategies toward aminotriazoles **15a-w** was dictated by unequal reactivity and different physicochemical properties of starting materials (carboxylic acids and their derivatives). This allowed to access aminotriazoles possessing aromatic, hetero-aromatic, aliphatic, and cycloaliphatic substituents of different size and electronic properties in 3-position of the triazole core. Additionally, the exocyclic primary amino group of two aminotriazoles **15a** and **15v** was varied using a reductive amination



Scheme 3. (a) DMF-DMA, neat, reflux, 16 h, **26a** 86%, **26b** 97%, **26c** 96%, **26d** 73%, **26e** 85%, **26f** 96%, **26g** 57%; (b) CH₃COONH₄, CH₃COOH, reflux, 16 h, **27a** 68%, **27b** 80%, **27c** 84%, **27d** 82%, **27e** 68%, **27f** 83%, **27g** 67%; (c) NH₂NH₂·H₂O, neat, reflux, 3 h, **28a** 83%, **28b** 70%, **28c** 87%, **28d** 72%, **28e** 78%, **28f** 80%, **28g** 87%; (d) 1. *S*-methylisothiuronium sulfate, EtOH/H₂O, reflux, 4 d, 2. KOH, EtOH/H₂O, reflux 3 h, **29a** 47%, **29b** 41%, **29c** 55%, **29d** 44%, **29e** 58%, **29f** 46%, **29g** 20%.

reaction with benzaldehyde affording compounds **19a** and **19v** bearing an extended exocyclic amino group (Scheme 1).

To access *1H*-1,2,4-triazol-5-amines **24a-d** exhibiting a quinoxalin-2-yl moiety as an alternative substituent in 3-position of the triazole core, synthesis shown in Scheme 2 was performed. This extension of the pyridyl moiety might lead to additional interactions with S1' and S2-S3 binding sites of FXIIa or thrombin and improve the compounds' affinity or selectivity e.g., toward FXIIa over thrombin, as thrombin exhibits a more narrow S2 binding site.^[3f,14] For this, commercially available β-ketoesters **20a-c** were brominated and then condensed with the symmetric *o*-phenylenediamines to afford fused heterocyclic esters **22a-d**.^[15] Esters **22a-d** were then converted into hydrazides **23a-d**, the consecutive treatment of which with *S*-methylisothiuronium sulfate and KOH afforded *1H*-1,2,4-triazol-5-amines **24a-d**.

With the same purpose to access fragments capable of reaching the enzymes' S1' and/or S2-S3 binding sites, aminotriazoles **29a-g**, possessing an extended pyridyl-moiety, were synthesized as shown in Scheme 3. For this purpose, condensation of ketones **25a-g** with *N,N*-dimethylformamide dimethyl acetal (DMF-DMA) was performed to get enaminones **26a-g**, which then reacted in a three-component cyclocondensation reaction with a β-ketoester and ammonium acetate affording substituted pyridines **27a-g**.^[16] Then, intermediates **27a-g** were treated with hydrazide monohydrate to produce hydrazides **28a-g**, which subsequently were converted into *1H*-1,2,4-triazol-5-amines **29a-g** using *S*-methylisothiuronium sulfate and KOH.

Other *1H*-1,2,4-triazol-5-amines used for the subsequent microscale parallel synthesis were available from our in-house library of aminoazoles prepared as previously reported.^[3f,17]

Microscale Parallel Synthesis and Screening

For the actual microscale parallel synthesis, 47 different 1*H*-1,2,4-triazol-5-amines were coupled with two selected carboxylic acids, namely (5)-1,2,3,4-tetrahydronaphthalene-1-carboxylic acid (30) and 2-iodophenylacetic acid (31), in a 96-well plate.

The carboxylic acids 30 and 31 were selected due to their unique structural features allowing, on the one hand, to access inhibitors with an improved selectivity toward FXIIa^[3f,18] and, on the other hand, to simplify the analysis of the microscale reaction mixtures by semi-^q1*H*-NMR. The proton signals of the methine group of 30 and of the methylene bridge of 31 are characteristic, do not overlap with other signals, and experience a low-field shift upon successful coupling reaction (e.g., the exemplary microscale reaction mixture shown in Figure 6). Moreover, both carboxylic acids being connected to the aminotriazoles, add three-dimensional character to the resulting molecules thereby improving their drug-like properties.

Right after the reaction was finished (3 h), 20 μ L of the reaction mixture was taken and diluted 1/100 with DMSO (solution A). Solution A was stored at -20°C until the subsequent biological activity screening, whereas the rest of the reaction mixture (100 μ L) was diluted with 600 μ L DMSO-*d*₆ (solution B) and submitted directly for semi-^q1*H*-NMR to determine the reaction conversion. The % of each aminotriazole conversion (94 microscale reactions) into the corresponding amide is shown in Figure 7. In general, the majority of aminotriazoles were successfully converted into desired *N*-acylated products with only a few showing low conversion under applied conditions. The average conversion of aminotriazoles into the corresponding amides was higher for tetrahydronaphthalene-1-carboxylic acid compared to 2-iodophenylacetic acid (Figure 7). Sufficient conversion was observed in 90 of 94 microscale reactions allowing further biological activity screening of 90 formed acylated aminotriazoles. Reaction mixtures with a conversion rate < 10% were excluded.

After the reaction conversion was determined by the analysis of the NMR spectrum of each reaction mixture, the concentration of the acylated product in solution A was calculated. The frozen samples (solution A) were thawed and diluted a second time with a calculated amount of DMSO to set the concentration of each acylated product to 76 μ mol/L. This allowed screening of the generated library of 90 acylated products against FXIIa and thrombin at two certain concentrations 1 μ M and 100 nM. For this purpose, the % of enzymes' inhibition was estimated utilizing fluorogenic substrates (Figure 8).

The medium-throughput screening revealed that the majority of *N*-acylated aminotriazoles, generated in microscale reactions, significantly inhibited the FXIIa enzymatic activity at 1 μ M (Figure 8 A, B). The inhibition was dose-dependent and clearly decreased upon compounds' concentration reduction to 100 nM. Screening showed that compounds possessing aminotriazole moiety (FR1) substituted with 3-methylquinoxalin-2-yl (A1), quinoline-2-yl (A5), pyridin-2-yl (D7), and pyrazin-2-yl (C11) caused more than 50% of FXIIa activity inhibition at 100 nM. Compounds bearing these aminotriazole fragments were

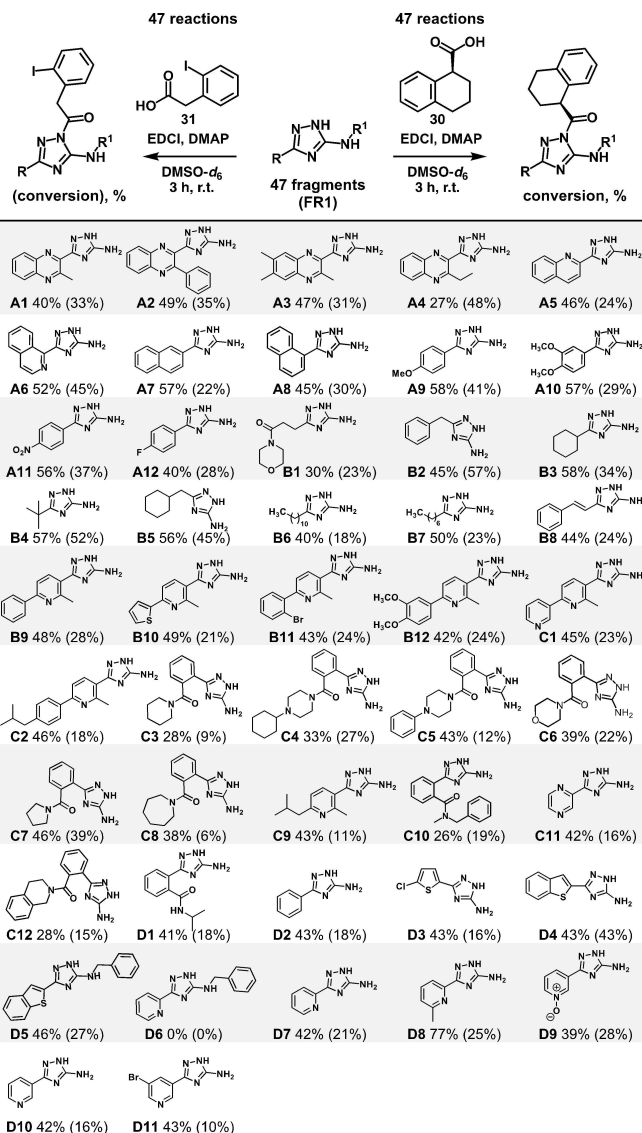


Figure 7. The structures of 1*H*-1,2,4-triazol-5-amines (47 fragments, FR1) used for the microscale amide coupling reactions with carboxylic acids 30 and 31; for each of 94 microscale reactions, % of aminotriazole conversion into corresponding amide is shown for carboxylic acid 30 (values without parentheses) and for carboxylic acid 31 (values in the parentheses); the letter code (A1-D11) indicates the position of the well in the 96-well plate.

denoted as hit compounds with expected IC_{50} values of ≤ 100 nM toward FXIIa. Significantly fewer compounds were found to inhibit thrombin (Figure 8). This was, however, expected as the employed acyl building blocks (FR2) are known to be more selective toward FXIIa.^[3f] Nevertheless, the screening allowed to identify four potentially interesting thrombin inhibitors such as compounds comprising isoquinolin-1-yl (A6), pyrazin-2-yl (C11), quinoline-2-yl (A5), and benzo[*b*]thiophen-2-yl (D5) fragments. Among them, aminotriazole exhibiting isoquinolin-1-yl moiety and acylated with (5)-1,2,3,4-tetrahydronaphthalene-1-carboxylic acid (A6) was expected to be the most potent thrombin inhibitor as it showed the highest

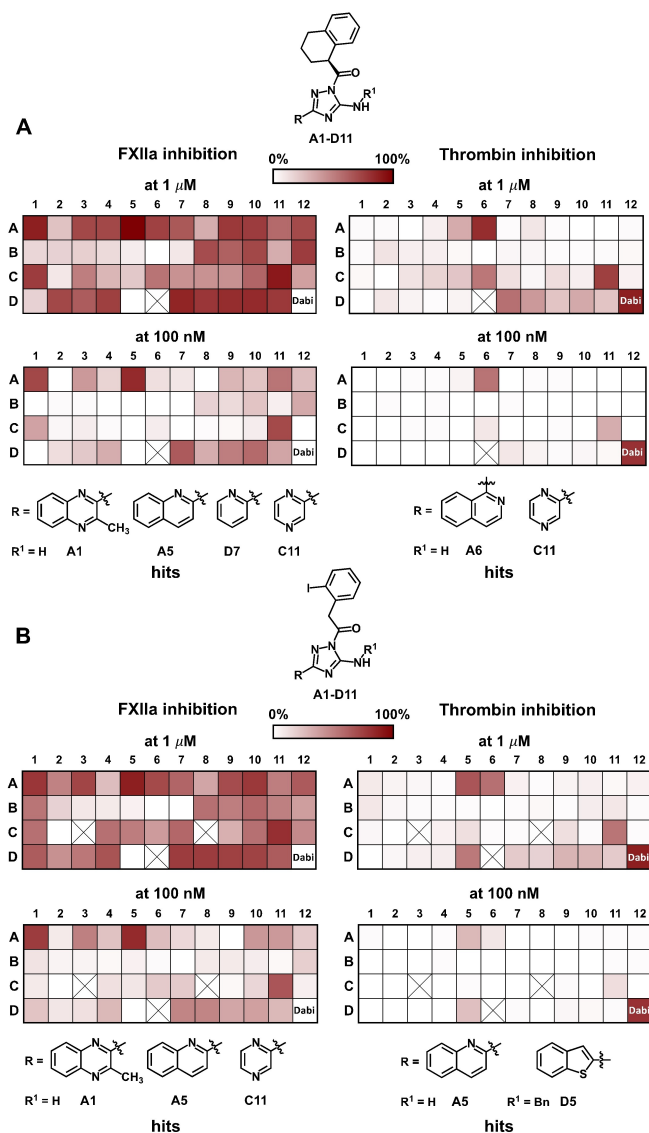


Figure 8. Library of 90 N-acylated 1*H*-1,2,4-triazol-5-amines screened against FXIIa and thrombin: 46 aminotriazole fragments possessed the acyl moiety of acid **30** (A) and 44 aminotriazole fragments of acid **31** (B). Well numbers (A1-D11) correspond to the structures shown in Figure 7. The extent of the enzymes' inhibition was quantified in percentage of residual protease activity. Crossed out cells indicate that no acylated product was formed (< 10%) according to semi- q^1 H-NMR and the mixture was not tested. Dabigatran (Dabi) was used as a positive control for thrombin inhibition and as a negative control for FXIIa inhibition.

thrombin inhibition among screened compounds (93% at 1 μ M and 62% at 100 nM).

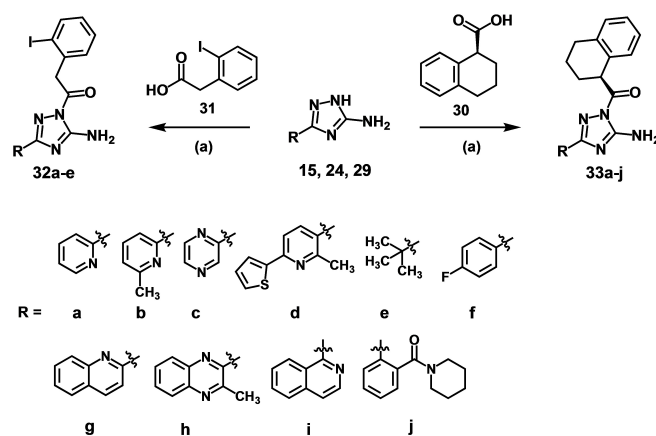
The screening also allowed to estimate another important aspect, the potential selectivity of the compounds. For instance, compounds possessing 3-methylquinoxalin-2-yl (A1) moiety were expected to be selective FXIIa inhibitors as they practically caused no thrombin inhibition, whereas isoquinolin-1-yl (A6)-substituted compounds were expected to inhibit thrombin rather more potently than FXIIa. Also, such compounds bearing, for instance, a pyrazin-2-yl (C11) moiety might exhibit dual FXIIa and thrombin inhibition.

Conventional Synthesis and Structure of Acylated Aminotriazoles

Based on the screening results of the microscale reaction mixtures, the acylated 1*H*-1,2,4-triazol-5-amines were clustered according to their ability to inhibit FXIIa and thrombin into four groups, namely high-, medium-, low-, and inactive inhibitors. To validate the parallel synthesis-based screening approach, apart from the most promising hit compounds, representatives of each activity cluster have been selected and synthesized, using the conventional synthetic method shown in Scheme 4. For this, aminotriazoles **15**, **24**, and **29** were subjected to amide coupling reactions with carboxylic acids **30** and **31** to afford desired N-acylated products **32 a–e** and **33 a–j**.

Before further progressing to the biological activity testing of pure compounds, their structure should have been explicitly confirmed. Exhibiting annular tautomerism, 1,2,4-triazol-5-amines exist in three tautomeric forms.^[17a] Therefore, the acylation of 1,2,4-triazol-5-amines may theoretically result in four acylated regioisomers, three of which arise from the annular tautomers and one from the possible acylation of the primary exocyclic amino group. To unambiguously prove the regioselectivity of the acylation process, we performed the X-ray crystallographic analysis of the reaction product **33 g** (Figure 9).

The X-ray analysis confirmed that the synthesized acylated aminotriazole **33 g** possess the acyl moiety in the N1-position of its triazole core. Also, the absolute configuration of the asymmetric C-atom of the acyl moiety was confirmed to be (*S*)-configured. Concerning other structural features, it is worth mentioning that the aromatic quinoline and aminotriazole moieties of **33 g** are practically coplanar, whereas the compound's (*S*)-1,2,3,4-tetrahydronaphthoyl fragment is out of their plane. The cyclohexene ring adopts a half-chair conformation and adds certain three-dimensional properties to the molecule. Interestingly, in the crystal packing, two different half-chair conformers of **33 g** were observed (Supporting Information, Figure S1).



Scheme 4. (a) EDCI, DMAP, pyridine, DMF, 0 °C to r.t., 4 h, **32 a** 61%, **32 b** 76%, **32 c** 65%, **32 d** 99%, **32 e** 78%, **33 a** 75%, **33 b** 79%, **33 c** 23%, **33 d** 87%, **33 e** 84%, **33 f** 93%, **33 g** 44%, **33 h** 32%, **33 i** 57%, **33 j** 49%.

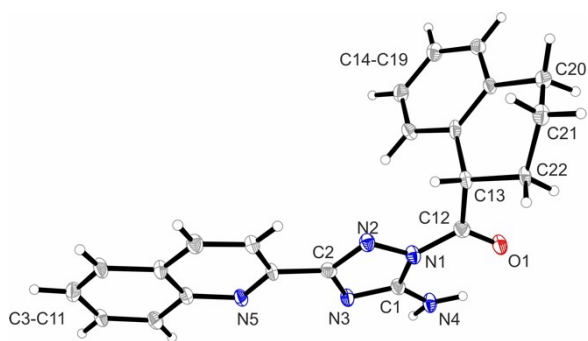


Figure 9. X-ray crystal structure of FXIIa inhibitor N-acylated 1*H*-1,2,4-triazol-5-amine **33g** displaying the thermal ellipsoids at the 50% probability level.

Serine Protease Inhibition by Pure Acylated Aminotriazoles

Selected from the microscale reactions screening, pure acylated 1*H*-1,2,4-triazol-5-amines (Scheme 4) were tested for their ability to inhibit the proteolytic activity of two main targeted enzymes FXIIa and thrombin (Table 2). Also, the compounds' selectivity against two structurally related serine proteases namely FXa and trypsin was studied (Table 2).

Performed enzymatic assays showed that those compounds, which significantly reduced the enzymatic activity in the screening, appeared to be active inhibitors of FXIIa and/or thrombin. E.g., aminotriazoles **32a–c**, and **33a,c,g,h**, which inhibited FXIIa activity by more than 50% at 100 nM in crude mixtures, showed the IC_{50} values toward FXIIa close to 100 nM or lower when

tested as pure compounds (Table 2). Among them, aminotriazole **33g** acylated with tetrahydronaphthalene-1-carboxylic acid and possessing quinolinyl moiety in 3-position of its triazole core was found to be the most potent FXIIa inhibitor with the IC_{50} = 33 nM, which is in a good agreement with its 94% of FXIIa inhibition (at 100 nM) in screening. Similarly, isoquinoline derivative **33i**, being the most potent thrombin inhibitor in the screening (62% at 100 nM), indeed showed the lowest IC_{50} value of 38 nM toward thrombin (Table 2).

Tests of pure compounds also confirmed that the developed screening method allows not only to find potent compounds but also to differentiate and discard low active and inactive inhibitors. For instance, aminotriazoles **32d,e**, and **33e,f,j** showed low activity in the microscale reactions screening and subsequently were proved to be only micromolar inhibitors or no inhibitors of FXIIa and thrombin when tested as pure compounds (Table 2). Additionally, tests of individual compounds proved that the developed screening method can efficiently predict compounds' selectivity. Thus, for instance, aminotriazoles **32c** and **33g** potentially inhibited FXIIa at 100 nM in the screening by 75% and 94%, respectively, showing subsequently the IC_{50} values of 65 nM and 33 nM, respectively (Table 2). At the same time, being screened against thrombin as crude mixtures, these two compounds inhibited thrombin by 15% and 5%, respectively, subsequently showing thrombin inhibition in the micromolar range as pure compounds (Table 2). Also, aminotriazole **33c**, which inhibited both FXIIa and thrombin during the screening (80% and 36% at 100 nM, respectively), was proved to be a dual inhibitor with IC_{50} = 106 nM (FXIIa) and 143 nM (thrombin) (Table 2).

Interestingly, 2-iodophenylacetic acid derivatives **32a–d** appeared to be more potent and selective FXIIa inhibitors than their counterparts **33a–c** possessing *S*-configured tetrahydronaphthoyl moiety (Table 2). This finding once again underlines that the structure of both fragments, aminotriazole core (FR1) and the acyl moiety (FR2) influences the compounds' inhibitory properties. It should also be noted that synthesized acylated aminotriazoles showed no off-targeting effect against two other serine proteases (IC_{50} > 5 μ M), FXa and trypsin, despite these enzymes' structural similarity with FXIIa and thrombin.^[14,19]

Post-Screening Optimization

Although compounds identified in the screening demonstrated promising inhibitory activity toward FXIIa and thrombin, there was still room for improvement, especially in terms of compounds' selectivity. We, therefore, designed post-screening structural modifications of the most promising N-acylated aminotriazoles. Particularly, the necessity of the methyl group on 3-methylquinoxalin-2-yl moiety of compound **33h** (122 nM inhibitor of FXIIa) was questioned. Its formal removal was suggested to be beneficial as structurally related compounds **33c** and **33g** having no such substituent were active FXIIa inhibitors (Table 2). Also, the analogs of aminotriazole **33h**, bearing the phenyl (A2) or the ethyl (A4) moiety in 3-position of

Table 2. Inhibition properties of acylated 1,2,4-triazol-5-amines **32a–e** and **33a–j** toward FXIIa, thrombin, FXa, and trypsin.

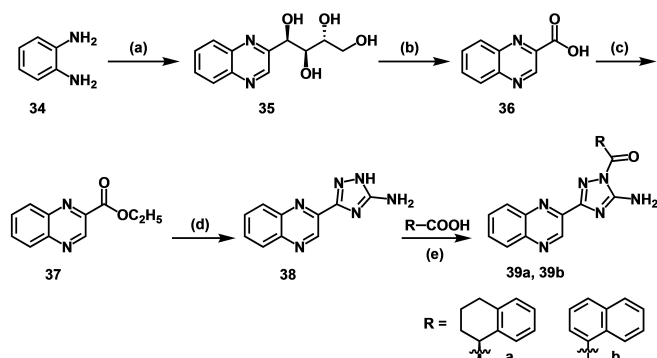
Cpd.	Inhibition @100 nM [in MTS] ^[a]		$IC_{50} \pm SD$ (nM) ^[b] Serine Protease			
	FXIIa	FIIa	FXIIa	FIIa	FXa	Tryps
32a	54%	2%	62 ± 22	1819 ± 155	> 5000	> 5000
32b	54%	0%	73 ± 22	> 5000	> 5000	> 5000
32c	75%	15%	65 ± 9	1694 ± 167	> 5000	> 5000
32d	8%	0%	716 ± 82	> 5000	> 5000	> 5000
32e	3%	1%	> 5000	> 5000	> 5000	> 5000
33a	73%	10%	134 ± 7	421 ± 2	> 5000	> 5000
33b	36%	5%	214 ± 35	819 ± 15	> 5000	> 5000
33c	80%	36%	106 ± 13	143 ± 5	> 5000	> 5000
33d	26%	0%	1135 ± 334	> 5000	> 5000	> 5000
33e	0%	1%	> 5000	> 5000	> 5000	> 5000
33f	29%	0%	~2000	> 5000	> 5000	> 5000
33g	94%	5%	33 ± 1	1013 ± 155	> 5000	> 5000
33h	81%	0%	122 ± 35	> 5000	> 5000	> 5000
33i	14%	62%	547 ± 58	38 ± 9	> 5000	> 5000
33j	8%	1%	1520 ± 182	5700 ± 330	> 5000	> 5000
Dabi	–1%	91%	> 5000	6.4 ± 0.4	34% ^[c]	59% ^[d]
Rivar	–1%	1%	> 5000	> 5000	0.7 ± 0.1	> 5000

Dabi-dabigatran, Rivar-rivaroxaban, Tryps-trypsin; ^[a] enzyme inhibition % by microscale reaction mixture (crude) in medium-throughput screening (MTS); ^[a], ^[b] measurements were performed in triplicate; the substrate concentration $[S]_0$ = 25 μ M; measured FXIIa K_m = 167 ± 4 μ M for Boc-Gln-Gly-Arg-AMC substrate; measured thrombin K_m = 18 ± 1 μ M for Boc-Val-Pro-Arg-AMC substrate. The K_i -values couldn't be directly withdrawn from the Cheng-Prusoff equation in this case due to the enzyme-inhibitor covalent interaction; ^[c] inhibition % at 1 μ M; ^[d] inhibition % at 5 μ M.

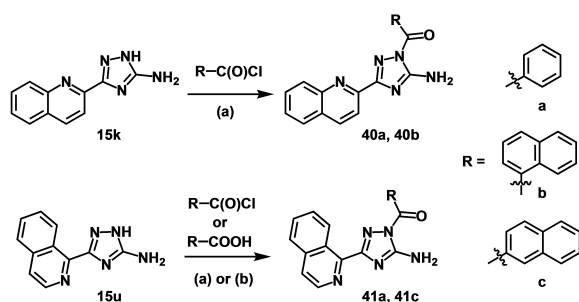
their quinoxaline scaffold instead of the methyl group, were low active FXIIa inhibitors (Figure 8).

Apart from that, the FXIIa inhibitory activity of the quinoline derivative **33 g** (FXIIa IC_{50} = 33 nM) might be further improved upon its acyl moiety replacement with a more suitable variant. For instance, α -naphthoyl moiety, previously found as a promising acyl fragment,^[37] could increase the compound's ability to inhibit FXIIa. Similarly, the thrombin inhibitory activity of isoquinoline-derived compound **33 i** (FIIa IC_{50} = 33 nM) might be improved upon its acyl moiety replacement with a fragment better fitting into the active site of thrombin. E.g., benzoyl and β -naphthoyl acyl fragments were previously shown to be favorable for thrombin inhibition.^[37]

To perform the formal removal of the methyl group of **33 h** and access compounds exhibiting a quinoxaline scaffold, synthesis shown in Scheme 5 was performed. For this purpose, *o*-phenylenediamine was condensed with D-fructose giving substituted quinoxaline **35**, the tetraol side chain of which was then oxidized accessing quinoxaline-2-carboxylic acid (**36**).^[20] The acid was esterified yielding ester **37**, which was then converted into corresponding aminotriazole **38** using aminoguanidine hydrochloride. Finally, **38** was coupled with two carboxylic acids affording N-acylated aminotriazoles **39 a** and **39 b** (Scheme 5).



Scheme 5. (a) D-fructose, AcOH (10%), 80 °C, 18 h, **35** 40%; (b) H₂O₂ (30%), NaOH (10%), 60 °C, 3 h, **36** 59%; (c) SOCl₂, EtOH, reflux, 3 h, **37** 91%; (d) 1. aminoguanidine hydrochloride, KOH, EtOH, r.t., 3 h; 2. EtOH, 80 °C, 18 h; 3. EtOH/H₂O, 105 °C, 3 h, **38** 54%; (e) EDCl, DMAP, pyridine, DMF, 0 °C to r.t., 4 h, **39 a** 68%, **39 b** 76%.



Scheme 6. (a) THF/pyridine 7:2, 0 °C to r.t., 2.5–4 h, **40 a** 87%, **40 b** 77%, **41 a** 99%, (b) EDCl, DMAP, pyridine, DMF, 0 °C to r.t., 4 h, **41 c** 79%.

Quinoline and isoquinoline-derived aminotriazoles possessing alternative acyl fragments in *N*-1-position of their core scaffold were obtained as shown in Scheme 6. For this, either a direct acylation reaction with acid chlorides or an amide coupling reaction was utilized affording desired *N*-acylated compounds **40 a,b** and **41 a,c** (Scheme 6).

Acyated aminotriazoles **39–41** obtained in the post-screening optimization step were tested against FXIIa, thrombin, FXa, and trypsin (Table 3). The performed structural modifications generally improved parent compounds' inhibitory properties against targeted enzymes. Particularly, the formal removal of the methyl group of **33 h** resulted in a quinoxaline **39 a** showing a 3.7-fold improved FXIIa inhibitory activity (122 nM vs. 33 nM) without losing selectivity (Table 3). Further FXIIa inhibitory activity enhancement was reached when the (*S*)-tetrahydronaphthoyl fragment of **39 a** was replaced with the α -naphthoyl moiety (**39 b**). The resulting compound **39 b** demonstrated the lowest IC_{50} value of 7 nM against FXIIa without off-targeting other tested serine proteases (IC_{50} > 5 μ M, Table 3). Likewise, the replacement of the tetrahydronaphthoyl moiety of **33 g** (FXIIa IC_{50} = 33 nM) with the benzoyl (**40 a**) or the α -naphthoyl moiety (**40 b**) decreased the parent compound's FXIIa IC_{50} value to 13 nM and 8 nM, respectively. All three quinolines **33 g**, **40 a**, and **40 b**, however, showed some off-targeting effect toward thrombin thus being dual FXIIa and thrombin inhibitors (Table 2 and Table 3). The acyl moiety variation was also beneficial for the isoquinoline-derived thrombin inhibitor **33 i** (FIIa IC_{50} = 33 nM). The replacement of the original acyl moiety of **33 i** by the β -naphthoyl fragment (**41 c**) slightly improved the compound's inhibitory activity toward thrombin (**41 c**, FIIa IC_{50} = 25 nM) and made it a selective thrombin inhibitor (Table 3). It should, however, be noted that the β -naphthoyl fragment despite being a good fit for thrombin inhibition, forms the enzyme-acyl complex with a rather short half-life.^[37]

Table 3. Inhibition properties of acylated 1,2,4-triazol-5-amines **39–41** synthesized in the post-screening optimization.

Cpd.	$IC_{50} \pm SD$ [nM] ^[a]			
	Serine Protease		FXa	Trypsin
	FXIIa	FIIa		
39 a	33 ± 7	> 5000	> 5000	32% ^[c]
39 b	7 ± 1	> 5000	> 5000	> 5000
40 a	13 ± 2	124 ± 10	> 5000	> 5000
40 b	8 ± 2	348 ± 15	–	> 5000
41 a	236 ± 5	63 ± 1	> 5000	> 5000
41 c	> 5000	25 ± 1	> 5000	> 5000
Dabigatran	> 5000	6.4 ± 0.4	34% ^[b]	59% ^[c]
Rivaroxaban	> 5000	> 5000	0.7 ± 0.1	> 5000

^[a] measurements were performed in triplicate; the substrate concentration $[S]_0$ = 25 μ M; measured FXIIa K_m = 167 ± 4 μ M for Boc-Gln-Gly-Arg-AMC substrate; measured thrombin K_m = 18 ± 1 μ M for Boc-Val-Pro-Arg-AMC substrate. The K_i -values couldn't be directly withdrawn from the Cheng-Prusoff equation in this case due to the enzyme-inhibitor covalent interaction; ^[b] inhibition % at 1 μ M; ^[c] inhibition % at 5 μ M.

Anticoagulant Activity of Acylated Aminotriazoles

Selected acylated aminotriazoles were screened for their anticoagulant properties in two tests namely activated partial thromboplastin time (aPTT) and prothrombin time (PT). These tests allow distinguishing whether the intrinsic or the extrinsic blood coagulation pathway is affected by test compounds. The measurement results are shown in Figure 10.

In general, compounds showing the FXIIa and/or FIIa inhibitory activity influenced the plasma coagulation time in the aPTT test (Figure 10). Among them, dual FXIIa/thrombin ($IC_{50} = 106/143$ nM) inhibitor **33c** possessing a pyrazin-2-yl moiety in 3-position of its aminotriazole core and the 5-configured tetrahydronaphthoyl residue as an acyl fragment showed the highest (2.7-fold) prolongation of aPTT. Two quinoline-derived FXIIa inhibitors **40a** and **40b** (FXIIa $IC_{50} = 13$ nM and 8 nM, respectively) with moderate thrombin inhibitory properties (124 nM and 348 nM, respectively) also extended coagulation time 1.7–1.8-fold in aPTT test. Except for thrombin inhibitor **41c**, tested aminotriazoles had practically no influence on the PT. This implies that compounds predominantly affected the intrinsic pathway of the blood coagulation cascade having little to no influence on the extrinsic pathway. This finding is interesting and might be considered as a beneficial property of acylated aminotriazoles as inhibition of intrinsic pathway was recently recognized as a potentially safe approach in therapy of thrombosis.^[6a]

Mechanism of Inhibition

Based on the previous studies, synthesized N-acylated aminotriazoles were expected to inhibit FXIIa and thrombin via a covalent reversible mechanism.^[3c,f] To prove that the com-

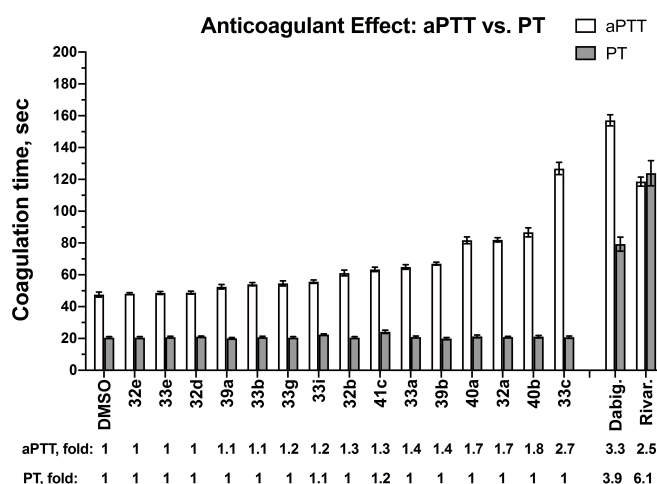


Figure 10. *In vitro* anticoagulant activity of selected acylated 1,2,4-triazol-5-amines screened at 200 μ M compared to that of dabigatran and rivaroxaban tested at 2 μ M. The activated partial thromboplastin time (aPTT) and prothrombin time (PT) are shown in seconds. The fold increase of aPTT and PT compared to the effect of DMSO is shown under the diagram. Tests were performed at least in triplicate, and the average with SD is given.

pounds undergo a covalent interaction with the targeted enzymes, we performed a mass-shift experiment with FXIIa and inhibitor **33g** (Figure 11).

In the experiment, native FXIIa was incubated for 15 min with the excess of inhibitor **33g** followed by size-exclusion chromatography (SEC) and the enzyme-inhibitor complex mass analysis using electrospray ionization mass spectrometry (ESI-MS). The measurement revealed that after the incubation, the initial mass of 29496.5 Da of FXIIa was shifted to 29654.7 Da. This mass shift ($\Delta m = 158.2$ Da) corresponds to the acyl moiety adduct of inhibitor **33g** to FXIIa confirming the covalent mechanism of FXIIa inhibition. As only a single acyl moiety transfer was observed, this process is limited to a specific site of the enzyme. Most likely, this site is the serine protease active site comprising the activated Ser195 capable of a nucleophilic attack on the inhibitor's carbonyl C-atom (Figure 11). Being acylated, serine protease temporarily (shown previously^[3f]) loses its proteolytic activity.

Conclusion

Collectively, we report a microscale parallel synthetic approach allowing for fast access to libraries of structurally diverse N-acylated aminotriazoles and screening of their inhibitory activity against selected serine proteases. This approach is simple, purification-free, and relies on inexpensive materials. Utilizing this method, a series of FXIIa and/or thrombin inhibitors were successfully identified. Subsequently performed post-screening structural optimization allowed to obtain more potent FXIIa and thrombin inhibitors, e.g. aminotriazoles **39b** (FXIIa $IC_{50} = 7$ nM) and **41c** (FIIa $IC_{50} = 25$ nM), which also showed no off-target effect against other physiologically relevant serine proteases. Some of the synthesized N-acylated aminotriazoles exhibited anticoagulant properties *in vitro* influencing the intrinsic blood

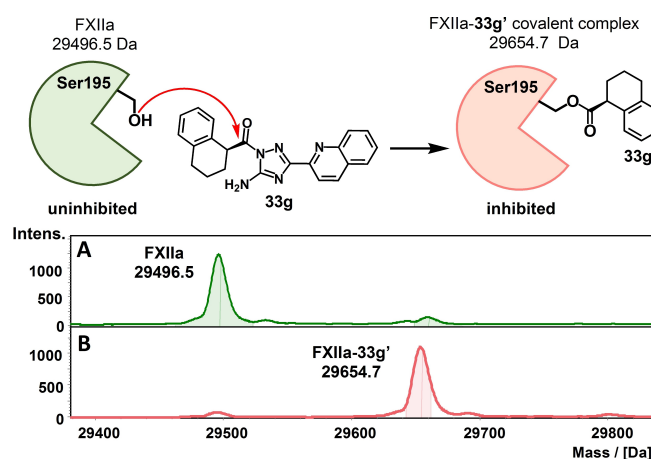


Figure 11. Deconvoluted SEC/ESI-TOF mass spectra of intact FXIIa (A) and the covalent complex FXIIa-**33g'** (B) formed after the FXIIa incubation (15 min) with the inhibitor **33g**. The peaks of interest are labelled with the corresponding deconvoluted masses. A mass shift of 158.2 Da is observed, which corresponds to the inhibitor's acyl moiety adduct. The schematic representation of FXIIa covalent inhibition by **33g** is also shown.

coagulation pathway but not the extrinsic coagulation. This is notable as extrinsic cascade triggered by tissue factor is physiologically important to prevent bleeding, whereas intrinsic pathway initiated by FXIIa is associated with thrombosis. Performed herein mechanistic studies of FXIIa inhibition suggested that synthesized N-acylated aminotriazoles are covalent inhibitors of FXIIa. Despite their prominent *in vitro* inhibitory activity against FXIIa and thrombin, synthesized compounds demonstrate weaker anticoagulant properties in plasma coagulation tests compared to dabigatran and rivaroxaban. Further structural variations on the 1*H*-1,2,4-triazol-5-amine-scaffold are required to obtain compounds with more potent anticoagulant properties before moving toward their *in vivo* tests.

Experimental Section

Chemistry, General. Unless otherwise mentioned, THF was dried with sodium/benzophenone and was freshly distilled before use. Thin layer chromatography (TLC): silica gel 60 F₂₅₄ plates (Merck). Flash chromatography (FC): silica gel 60, 40–63 μm (Macherey-Nagel). Reversed phase thin layer chromatography (RP-TLC): silica gel 60 RP-18 F₂₅₄S plates (Merck). Automatic flash column chromatography: Isolera One (Biotage); brackets include eluent, cartridge-type. Melting point (m.p.): melting point apparatus SMP 3 (Stuart Scientific), uncorrected. ¹H NMR (400 MHz), ¹H NMR (600 MHz), and ¹³C NMR (151 MHz): Agilent DD2 400 and 600 MHz spectrometers; chemical shifts (δ) are reported in ppm against the reference substance tetramethylsilane and calculated using the solvent residual peak of the undeuterated solvent. IR: IR Prestige-21 (Shimadzu). HRMS: MicroTOF-QII (Bruker). HPLC method to determine the purity of compounds: equipment 1: pump: L-7100, degasser: L-7614, autosampler: L-7200, UV detector: L-7400, interface: D-7000, data transfer: D-line, data acquisition: HSMS software (all from LaChrom, Merck Hitachi); equipment 2: pump: LPG-3400SD, degasser: DG-1210, autosampler: ACC-3000T, UV detector: VWD-3400RS, interface: Dionex UltiMate 3000, data acquisition: Chromeleon 7 (Thermo Fisher Scientific); column: LiChrospher 60 RP-select B (5 μm), LiChroCART 250–4 mm cartridge; flow rate: 1.0 mL/min; injection volume: 5.0 μL; detection at λ=210 nm; solvents: A: demineralized water with 0.05% (v/v) trifluoroacetic acid, B: acetonitrile with 0.05% (v/v) trifluoroacetic acid; gradient elution (% A): 0–4 min: 90%; 4–29 min: gradient from 90 to 0%; 29–31 min: 0%; 31–31.5 min: gradient from 0 to 90%; 31.5–40 min: 90%.

Synthesis of compounds **13a–d**, **15b**, and **15t** was previously reported by us.^[30] ¹H and ¹³C NMR spectra of all synthesized compounds, synthetic procedures and analytical data for compounds **13e**, **15a–s**, **15u–w**, **17u**, **18u,v**, **19a,v**, **22a–d**, **23a–d**, **24a–d**, **26a–g**, **27a–g**, **28a–g**, **29a–g**, and **35–38** are given in the Supporting Information.

1-(5-Amino-3-(pyridin-2-yl)-1*H*-1,2,4-triazol-1-yl)-2-(2-iodophenyl)ethan-1-one (32a). Triazole amine **15a** (100 mg, 621 μmol), 2-(2-iodophenyl)acetic acid (**31**, 163 mg, 621 μmol, 1.0 eq.), EDCI·HCl (238 mg, 1.24 mmol, 2.0 eq.) and DMAP (152 mg, 1.24 mmol, 2.00 eq.) were dissolved in DMF (4 mL, dry) and the reaction mixture stirred at 0 °C for 1 h and further 2 h at r.t.. The mixture was diluted with H₂O (100 mL) filtrated and the residue washed with H₂O and dried *in vacuo*. The crude product was purified by flash-column chromatography (DCM/ACN=9/1→75/25) to yield **32a** as a colourless solid (152 mg, 375 μmol, 61%). M.p. > 300 °C. TLC: R_f=0.34 (DCM/MeOH=9/1). ¹H-NMR (600 MHz, DMSO-*d*₆, 299 K): δ (in ppm)=8.70 (ddd, *J*=4.7, 1.8, 0.9 Hz, 1H, 6-*H*_{pyridyl}), 8.05 (dt, *J*=7.9, 1.1 Hz, 1H, 3-*H*_{pyridyl}), 7.94

(td, *J*=7.7, 1.8 Hz, 1H, 4-*H*_{pyridyl}), 7.89 (dd, *J*=7.9, 1.3 Hz, 1H, 3-*H*_{2-iodophenylacetyl}), 7.70 (bs, 2H, NH₂), 7.52–7.47 (m, 2H, 5-*H*_{pyridyl}/6-*H*_{2-iodophenylacetyl}), 7.41 (td, *J*=7.4, 1.3 Hz, 1H, 5-*H*_{2-iodophenylacetyl}), 7.08 (td, *J*=7.6, 1.7 Hz, 1H, 4-*H*_{2-iodophenylacetyl}), 4.60 (s, 2H, CH₂). ¹³C-NMR (151 MHz, DMSO-*d*₆, 299 K): δ (in ppm)=170.8 (1 C, C=O), 159.4 (1 C, 3-*C*_{triazolyl}), 157.5 (1 C, 5-*C*_{triazolyl}), 149.8 (1 C, 6-*C*_{pyridyl}), 148.9 (1 C, 2-*C*_{pyridyl}), 138.8 (1 C, 3-*C*_{2-iodophenylacetyl}), 137.4 (1 C, 1-*C*_{2-iodophenylacetyl}), 137.1 (1 C, 4-*C*_{pyridyl}), 131.9 (1 C, 6-*C*_{2-iodophenylacetyl}), 129.3 (1 C, 4-*C*_{2-iodophenylacetyl}), 128.4 (1 C, 5-*C*_{2-iodophenylacetyl}), 124.8 (1 C, 5-*C*_{pyridyl}), 122.5 (1 C, 3-*C*_{pyridyl}), 102.1 (1 C, 2-*C*_{2-iodophenylacetyl}), 46.5 (1 C, CH₂). IR (neat): ν̄ [cm⁻¹]=1287, 1634, 1713, 2980, 2999, 3028, 3271, 3456. HRMS (APCI): *m/z*=406.0159 calculated for C₁₅H₁₃N₅O⁺ [M+H]⁺, found: 406.0141. HPLC: t_R=17.6 min, purity: 99.9%.

1-(5-Amino-3-(6-methylpyridin-2-yl)-1*H*-1,2,4-triazol-1-yl)-2-(2-iodophenyl)ethan-1-one (32b). Compound **15e** (100 mg, 571 μmol, 1.0 eq.), 2-iodophenylacetic acid (150 mg, 571 μmol), DMAP (140 mg, 1.14 mmol, 2.0 eq.) and EDCI·HCl (219 mg, 1.14 mmol, 2.0 eq.) were dissolved in DMF (7 mL) and pyridine (2 mL, both dry) under nitrogen atmosphere at 0 °C. The solution was stirred at 0 °C for 1 h and then at r.t. for 4 h. The reaction mixture was poured into cold H₂O and stored at 4 °C for 15 min. The formed precipitate was filtered off, washed with H₂O and Et₂O and purified via flash-column chromatography (DCM/MeOH=1/0→95/5). The product was obtained as a colourless solid (182 mg, 433 μmol, 76%). M.p.=213.5 °C. TLC: R_f=0.44 (DCM/MeOH=20/1). ¹H-NMR (600 MHz, DMSO-*d*₆, 299 K): δ (in ppm)=7.89 (d, *J*=7.6 Hz, 1H, 3-*H*_{phenylacetyl}), 7.87 (d, *J*=7.7 Hz, 1H, 6-*H*_{pyridyl}), 7.82 (dd, *J*=7.7 Hz, 1H, 5-*H*_{pyridyl}), 7.67 (s, 2H, -NH₂), 7.48 (d, *J*=7.5 Hz, 1H, 6-*H*_{phenylacetyl}), 7.41 (t, *J*=7.6, 7.5 Hz, 1H, 5-*H*_{phenylacetyl}), 7.36 (d, *J*=7.7 Hz, 1H, 4-*H*_{pyridyl}), 7.08 (dd, *J*=7.6 Hz, 1H, 4-*H*_{phenylacetyl}), 4.60 (s, 2H, -CH₂-), 2.55 (s, 3H, -CH₃). ¹³C-NMR (151 MHz, DMSO-*d*₆, 299 K): δ (in ppm)=170.7 (1 C, C=O), 159.6 (1 C, 3-*C*_{triazolyl}), 158.2 (1 C, 3-*C*_{pyridyl}), 157.5 (1 C, 5-*C*_{triazolyl}), 148.3 (1 C, 1-*C*_{pyridyl}), 138.7 (1 C, 3-*C*_{phenylacetyl}), 137.4 (1 C, 1-*C*_{phenylacetyl}), 137.2 (1 C, 5-*C*_{pyridyl}), 131.9 (1 C, 6-*C*_{phenylacetyl}), 129.3 (1 C, 4-*C*_{phenylacetyl}), 128.3 (1 C, 5-*C*_{phenylacetyl}), 124.2 (1 C, 4-*C*_{pyridyl}), 120.3 (1 C, 6-*C*_{pyridyl}), 102.2 (1 C, 2-*C*_{phenylacetyl}), 46.5 (1 C, -CH₂-), 24.1 (1 C, -CH₃). IR (neat): ν̄ [cm⁻¹]=3445, 3051, 2920, 1724, 1627, 1528, 1466, 1392, 1366, 1265, 1169, 1003, 1049, 752. HRMS (APCI): *m/z*=420.0316 calculated for C₁₆H₁₅N₅O⁺ [M+H]⁺, found: 420.0314. HPLC: t_R=17.3 min, purity: 92.5%.

1-(5-Amino-3-(pyrazin-2-yl)-1*H*-1,2,4-triazol-1-yl)-2-(2-iodophenyl)ethan-1-one (32c). 3-(Pyrazin-2-yl)-1*H*-1,2,4-triazol-5-amine (81 mg, 500 μmol, 1.0 eq.), 2-iodophenylacetic acid (130 mg, 496 μmol, 1.0 eq.), DMAP (123 mg, 1.01 mmol, 2.0 eq.) and EDCI·HCl (191 mg, 999 μmol, 2.0 eq.) were dissolved in DMF (7 mL, dry) and pyridine (2 mL, dry) at 0 °C. The solution was stirred at 0 °C for 1 h and then at r.t. for 4 h. Then, the mixture was poured into cold H₂O and stored at 4 °C for 15 min. The precipitate was filtered off and washed with H₂O and Et₂O. The product was obtained after purification via flash-column chromatography (DCM/MeOH=1/0→95/5) as a colourless solid (133 mg, 326 μmol, 65%). M.p. > 235 °C (decomp.). TLC: R_f=0.43 (DCM/MeOH=20/1). ¹H-NMR (600 MHz, DMSO-*d*₆, 299 K): δ (in ppm)=9.22 (s, 1H, 3-*H*_{pyrazin}), 8.79 (d, *J*=2.5 Hz, 1H, 6-*H*_{pyrazin}), 8.76 (d, *J*=2.5 Hz, 1H, 5-*H*_{pyrazin}), 7.89 (d, *J*=7.9 Hz, 1H, 3-*H*_{phenylacetyl}), 7.80 (bs, 2H, -NH₂), 7.48 (d, *J*=7.6 Hz, 1H, 6-*H*_{phenylacetyl}), 7.42 (dd, *J*=7.6 Hz, 1H, 5-*H*_{phenylacetyl}), 7.09 (dd, *J*=7.9, 7.6 Hz, 1H, 4-*H*_{phenylacetyl}), 4.61 (s, 2H, -CH₂-). ¹³C-NMR (151 MHz, DMSO-*d*₆, 299 K) δ (in ppm)=170.7 (1 C, C=O), 157.7 (1 C, 3-/5-*C*_{triazolyl}), 157.5 (1 C, 3-/5-*C*_{triazolyl}), 145.7 (1 C, 5-*C*_{pyrazin}), 144.8 (1 C, 6-*C*_{pyrazin}), 144.5 (1 C, 2-*C*_{pyrazin}), 143.4 (1 C, 3-*C*_{pyrazin}), 138.8 (1 C, 3-*C*_{iodophenylacetyl}), 137.2 (1 C, 1-*C*_{iodophenylacetyl}), 131.9 (1 C, 6-*C*_{iodophenylacetyl}), 129.3 (1 C, 4-*C*_{iodophenylacetyl}), 128.4 (1 C, 5-*C*_{iodophenylacetyl}), 102.7 (1 C, 2-*C*_{iodophenylacetyl}), 46.5 (1 C, -CH₂-). IR (neat): ν̄ [cm⁻¹]=3437, 3048, 2913, 1717, 1639, 1543, 1466, 1393, 1366, 1265, 1145, 1011, 741.

HRMS (APCI): $m/z = 407.0112$ calculated for $C_{14}H_{12}N_6O^+$ [M+H]⁺, found: 407.0094. HPLC: $t_R = 18.3$ min, purity: 94.2%.

1-(5-Amino-3-(2-methyl-6-(thiophen-2-yl)pyridin-3-yl)-1H-1,2,4-triazol-1-yl)-2-(2-iodophenyl)ethan-1-one (32d). Compound **29f** (100 mg, 389 μ mol, 1.0 eq.), 2-iodophenylacetic acid (102 mg, 389 μ mol, 1.0 eq.), DMAP (95 mg, 777 μ mol, 2.0 eq.) and EDCI·HCl (149 mg, 777 μ mol, 2.0 eq.) were dissolved at 0 °C under nitrogen atmosphere and stirred at 0 °C for 1 h and then at r.t. for 4 h. Then, the mixture was poured into cold H₂O and stored at 4 °C for 15 min. The formed precipitate was filtered off and washed with H₂O and Et₂O. The product was purified via flash-column chromatography (DCM/MeOH = 1/0 → 95/5) and was obtained as a colourless solid (193 mg, 386 μ mol, 99%). M.p. = 190–200 °C. TLC: $R_f = 0.52$ (DCM/MeOH = 20/1). ¹H-NMR (600 MHz, DMSO-*d*₆, 299 K): δ (in ppm) = 8.32 (d, $J = 8.2$ Hz, 1H, 6-H_{pyridyl}), 7.90 (d, $J = 7.6$ Hz, 1H, 3-H_{phenylacetyl}), 7.88 (d, $J = 8.2$ Hz, 1H, 5-H_{pyridyl}), 7.85 (d, $J = 3.7$ Hz, 1H, 4-H_{thiophenyl}), 7.71 (s, 2H, -NH₂), 7.68 (d, $J = 5.0$ Hz, 1H, 2-H_{thiophenyl}), 7.48 (d, $J = 7.6$ Hz, 1H, 6-H_{phenylacetyl}), 7.42 (d, $J = 7.6$, 7.5 Hz, 1H, 5-H_{phenylacetyl}), 7.19 (dd, $J = 5.0$, 3.7 Hz, 1H, 3-H_{thiophenyl}), 7.08 (dd, $J = 7.6$, 7.5 Hz, 1H, 4-H_{phenylacetyl}), 4.60 (s, 2H, -CH₂-), 2.89 (s, 3H, -CH₃). ¹³C-NMR (151 MHz, DMSO-*d*₆, 299 K) δ (in ppm) = 170.6 (1 C, C=O), 158.8 (1 C, 3-/5-C_{triazolyl}), 156.9 (1 C, 3-/5-C_{triazolyl}), 156.6 (1 C, 2-C_{pyridyl}), 151.4 (1 C, 4-C_{pyridyl}), 144.0 (1 C, 1-C_{thiophenyl}), 138.8 (1 C, 3-C_{phenylacetyl}), 137.8 (1 C, 6-C_{pyridyl}), 137.4 (1 C, 1-C_{phenylacetyl}), 131.8 (1 C, 6-C_{phenylacetyl}), 129.3 (1 C, 4-C_{phenylacetyl}), 129.1 (1 C, 2-C_{thiophenyl}), 128.6 (1 C, 3-C_{thiophenyl}), 128.4 (1 C, 5-C_{phenylacetyl}), 126.0 (1 C, 4-C_{thiophenyl}), 122.9 (1 C, 1-C_{pyridyl}), 116.1 (1 C, 5-C_{pyridyl}), 102.1 (1 C, 2-C_{phenylacetyl}), 46.5 (1 C, -CH₂-), 25.3 (1 C, -CH₃). IR (neat): $\tilde{\nu}$ [cm⁻¹] = 3437, 3066, 2924, 1721, 1643, 1578, 1466, 1361, 1323, 1045, 1007, 837, 721. HRMS (APCI): $m/z = 502.0193$ calculated for $C_{20}H_{17}N_5O^+$ [M+H]⁺, found: 502.0189. HPLC: $t_R = 22.4$ min, purity: 93.7%.

1-(5-Amino-3-(tert-butyl)-1H-1,2,4-triazol-1-yl)-2-(2-iodophenyl)ethan-1-one (32e). Compound **15h** (80 mg, 571 μ mol, 1.0 eq.), 2-iodophenylacetic acid (150 mg, 571 μ mol, 1.0 eq.), DMAP (139 mg, 1.14 mmol, 2.0 eq.) and EDCI·HCl (219 mg, 1.14 mmol, 2.0 eq.) were dissolved in DMF (7 mL, dry) and pyridine (2 mL, dry) at 0 °C. The reaction solution was stirred at 0 °C for 1 h and then at r.t. for 4 h. The reaction mixture was poured into cold H₂O and stored at 4 °C for 15 min. The formed precipitate was filtered off and washed thoroughly with H₂O. The remaining product was dissolved in Et₂O, the solvent evaporated and dried *in vacuo*. The product was obtained as a colourless solid (173 mg, 449 μ mol, 78%). M.p. = 149.5 °C. TLC: $R_f = 0.49$ (DCM/MeOH = 20/1). ¹H-NMR (600 MHz, DMSO-*d*₆, 299 K): δ (in ppm) = 7.87 (d, $J = 7.6$ Hz, 1H, 3-H_{phenylacetyl}), 7.44 (m, 3H, -NH₂/6-H_{phenylacetyl}), 7.38 (t, $J = 7.6$ Hz, 1H, 5-H_{phenylacetyl}), 7.05 (t, $J = 7.6$ Hz, 1H, 4-H_{phenylacetyl}), 4.45 (s, 2H, -CH₂-), 1.28 (s, 9H, -(CH₃)₃). ¹³C-NMR (151 MHz, DMSO-*d*₆, 299 K): δ (in ppm) = 170.3 (1 C, C=O), 157.2 (1 C, 3-/5-C_{triazolyl}), 138.7 (1 C, 3-C_{phenylacetyl}), 137.4 (1 C, 1-C_{phenylacetyl}), 131.8 (1 C, 6-C_{phenylacetyl}), 129.2 (1 C, 4-C_{phenylacetyl}), 128.3 (1 C, 5-C_{phenylacetyl}), 103.3 (1 C, 2-C_{phenylacetyl}), 46.3 (1 C, -CH₂-), 32.5 (1 C, -C-(CH₃)₃), 28.6 (3 C, -C-(CH₃)₃). IR (neat): $\tilde{\nu}$ [cm⁻¹] = 3429, 2970, 1721, 1643, 1539, 1377, 1192, 1015, 914, 749, 649, 644. HRMS (APCI): $m/z = 385.0520$ calculated for $C_{14}H_{18}N_4O^+$ [M+H]⁺, found: 385.0522. HPLC: $t_R = 20.5$ min, purity: 96.5%.

(S)-(5-Amino-3-(pyridin-2-yl)-1H-1,2,4-triazol-1-yl)(1,2,3,4-tetrahydronaphthalen-1-yl)methanone (33a). Triazole amine **15a** (100 mg, 621 μ mol, 1.0 eq.), (S)-1,2,3,4-tetrahydronaphthalene-1-carboxylic acid (**30**, 109 mg, 621 μ mol, 1.0 eq.), EDCI·HCl (238 mg, 1.24 mmol, 2.0 eq.) and DMAP (152 mg, 1.24 mmol, 2.0 eq.) were dissolved in DMF (3 mL, dry) and the reaction mixture was stirred at 0 °C for 1 h and further 2 h at r.t.. The mixture was diluted with H₂O (100 mL, 0 °C) and the formed precipitation was filtrated off and washed with H₂O (10 mL). The residue was dried *in vacuo* to yield compound **33a** as a beige solid (148 mg, 463 μ mol, 75%). M.p. = 157–158 °C. TLC: $R_f = 0.61$ (DCM/MeOH = 9/1). ¹H-NMR (600 MHz,

DMSO-*d*₆, 299 K): δ (in ppm) = 8.69 (ddd, $J = 4.7$, 1.7, 0.7 Hz, 1H, 6-H_{pyridyl}), 8.05 (dt, $J = 7.8$; 1.0 Hz, 1H, 3-H_{pyridyl}), 7.94 (td, $J = 7.7$, 1.8 Hz, 1H, 4-H_{pyridyl}), 7.72 (bs, 2H, NH₂), 7.49 (ddd, $J = 7.6$, 4.7, 1.2 Hz, 1H, 5-H_{pyridyl}), 7.19–7.14 (m, 2H, 5-/6-H_{tetrahydronaphthyl}), 7.12–7.07 (m, 2H, 7-/8-H_{tetrahydronaphthyl}), 5.07 (t, $J = 6.4$ Hz, 1H, 2-H_{tetrahydronaphthyl}), 2.86–2.74 (m, 2H, 3-H_{tetrahydronaphthyl}), 2.25–2.17 (m, 1H, 1-H_{tetrahydronaphthyl}), 2.13–2.07 (m, 1H, 1-H_{tetrahydronaphthyl}), 1.94–1.86 (m, 1H, 4-H_{tetrahydronaphthyl}), 1.81–1.73 (m, 1H, 4-H_{tetrahydronaphthyl}). ¹³C-NMR (151 MHz, DMSO-*d*₆, 299 K): δ (in ppm) = 175.7 (1 C, C=O), 159.5 (1 C, 3-C_{triazolyl}), 157.9 (1 C, 5-C_{triazolyl}), 149.7 (1 C, 6-C_{pyridyl}), 148.9 (1 C, 2-C_{pyridyl}), 137.5 (1 C, 4a-C_{tetrahydronaphthyl}), 137.1 (1 C, 4-C_{pyridyl}), 133.1 (1 C, 8a-C_{tetrahydronaphthyl}), 129.3 (1 C, 8-C_{tetrahydronaphthyl}), 129.2 (1 C, 5-C_{tetrahydronaphthyl}), 126.8 (1 C, 6-C_{tetrahydronaphthyl}), 125.8 (1 C, 7-C_{tetrahydronaphthyl}), 124.8 (1 C, 5-C_{pyridyl}), 122.6 (1 C, 3-C_{pyridyl}), 43.2 (1 C, 2-C_{tetrahydronaphthyl}), 28.6 (1 C, 3-C_{tetrahydronaphthyl}), 26.3 (1 C, 1-C_{tetrahydronaphthyl}), 20.0 (1 C, 4-C_{tetrahydronaphthyl}). IR (neat): $\tilde{\nu}$ [cm⁻¹] = 1257, 1628, 1713, 2932, 2980, 3196, 3426, 3447. HRMS (APCI): $m/z = 320.1506$ calculated for $C_{18}H_{18}N_5O^+$ [M+H]⁺, found: 320.1517. HPLC: $t_R = 17.8$ min, purity: 97.5%.

(S)-(5-Amino-3-(6-methylpyridin-2-yl)-1H-1,2,4-triazol-1-yl)(1,2,3,4-tetrahydronaphthalen-1-yl)methanone (33b). Compound **15e** (80 mg, 457 μ mol, 1.0 eq.), (S)-1,2,3,4-tetrahydronaphthalene-1-carboxylic acid (80 mg, 457 μ mol, 1.0 eq.), DMAP (112 mg, 913 μ mol, 2.0 eq.) and EDCI·HCl (175 mg, 913 μ mol, 2.0 eq.) were dissolved in DMF (7 mL, dry) and pyridine (2 mL, dry) at 0 °C under nitrogen atmosphere. The solution was stirred at 0 °C for 1 h and then at r.t. for 4 h. The reaction mixture was poured into cold H₂O and stored at 4 °C for 15 min. The formed precipitate was filtered off and washed with H₂O thoroughly. The remaining solid was dried *in vacuo*, the product was obtained as a colourless solid (120 mg, 361 μ mol, 79%). M.p. = 176.5 °C. TLC: $R_f = 0.38$ (DCM/MeOH = 20/1). ¹H-NMR (600 MHz, DMSO-*d*₆, 299 K): δ (in ppm) = 7.86 (d, $J = 7.7$ Hz, 1H, 3-H_{pyridyl}), 7.81 (t, $J = 7.7$ Hz, 1H, 4-H_{pyridyl}), 7.70 (s, 2H, -NH₂), 7.35 (d, $J = 7.7$ Hz, 1H, 5-H_{pyridyl}), 7.20–7.13 (m, 2H, 5-/8-H_{tetrahydronaphthyl}), 7.12–7.05 (m, 2H, 6-/7-H_{tetrahydronaphthyl}), 5.08 (t, $J = 6.4$ Hz, 1H, 1-H_{tetrahydronaphthyl}), 2.86–2.74 (m, 2H, 4-H_{tetrahydronaphthyl}), 2.54 (s, 3H, -CH₃), 2.24–2.16 (m, 1H, 2a-H_{tetrahydronaphthyl}), 2.13–2.06 (m, 1H, 2b-H_{tetrahydronaphthyl}), 1.95–1.87 (m, 1H, 3a-H_{tetrahydronaphthyl}), 1.80–1.72 (m, 1H, 3b-H_{tetrahydronaphthyl}). ¹³C-NMR (151 MHz, DMSO-*d*₆, 299 K) δ (in ppm) = 175.7 (1 C, C=O), 159.7 (1 C, 3-C_{triazolyl}), 158.2 (1 C, 6-C_{pyridyl}), 157.9 (1 C, 5-C_{triazolyl}), 148.3 (1 C, 2-C_{pyridyl}), 137.5 (1 C, 4a-C_{tetrahydronaphthyl}), 137.2 (1 C, 3-C_{pyridyl}), 133.1 (1 C, 8'-C_{tetrahydronaphthyl}), 129.2 (1 C, 5-/8-C_{tetrahydronaphthyl}), 126.8 (1 C, 6-/7-C_{tetrahydronaphthyl}), 125.8 (1 C, 6-/7-C_{tetrahydronaphthyl}), 124.2 (1 C, 4-C_{pyridyl}), 119.8 (1 C, 5-C_{pyridyl}), 43.2 (1 C, 1-C_{tetrahydronaphthyl}), 28.6 (1 C, 4-C_{tetrahydronaphthyl}), 26.3 (1 C, 2-C_{tetrahydronaphthyl}), 24.1 (1 C, -CH₃), 20.0 (1 C, 3-C_{tetrahydronaphthyl}). IR (neat): $\tilde{\nu}$ [cm⁻¹] = 3453, 3017, 2936, 1709, 1647, 1574, 1466, 1362, 1273, 1153, 991, 745, 702. HRMS (APCI): $m/z = 334.1662$ calculated for $C_{19}H_{20}N_5O^+$ [M+H]⁺, found: 334.1661. HPLC: $t_R = 17.6$ min, purity: 99.3%.

(S)-(5-Amino-3-(pyrazin-2-yl)-1H-1,2,4-triazol-1-yl)(1,2,3,4-tetrahydronaphthalen-1-yl)methanone (33c). 3-(Pyrazin-2-yl)-1H-1,2,4-triazol-5-amine (**38** mg, 234 μ mol, 1.0 eq.), (S)-1,2,3,4-tetrahydronaphthalene-1-carboxylic acid (41 mg, 233 μ mol, 1.0 eq.), DMAP (60 mg, 491 μ mol, 2.1 eq.) and EDCI·HCl (89 mg, 464 μ mol, 2.0 eq.) were dissolved in DMF (3.5 mL, dry) and pyridine (1.0 mL, dry) under nitrogen atmosphere at 0 °C. The solution was stirred at 0 °C for 1 h and then at r.t. for 4 h. The reaction mixture was poured into cold H₂O and stored at 4 °C for 15 min. The formed precipitate was filtered off and washed thoroughly with H₂O. The remaining solid was dried *in vacuo*, the product was obtained as a colourless solid (18 mg, 55 μ mol, 23%). M.p. = 176.5 °C. TLC: $R_f = 0.47$ (DCM/MeOH = 20/1). ¹H-NMR (600 MHz, DMSO-*d*₆, 299 K): δ (in ppm) = 9.22 (s, 1H, 3-H_{pyrazine}), 8.78 (d, $J = 2.5$ Hz, 1H, 6-H_{pyrazine}), 8.76 (d, $J = 2.5$ Hz, 1H, 5-H_{pyrazine}), 7.82 (s, 2H, -NH₂), 7.20–7.13 (m, 2H, 5-H_{tetrahydronaphthyl}), 6'-/7'-H_{tetrahydronaphthyl}, 7.13–7.07 (m, 2H, 8-H_{tetrahydronaphthyl}), 6'-/7'-H_{tetrahydronaphthyl}.

$H_{\text{tetrahydronaphthoyl}}$, 5.06 (t, $J=6.3$ Hz, 1H, 1- $H_{\text{tetrahydronaphthoyl}}$), 2.86–2.72 (m, 2H, 4- $H_{\text{tetrahydronaphthoyl}}$), 2.25–2.16 (m, 1H, 2a- $H_{\text{tetrahydronaphthoyl}}$), 2.15–2.08 (m, 1H, 2b- $H_{\text{tetrahydronaphthoyl}}$), 1.93–1.85 (m, 1H, 3a- $H_{\text{tetrahydronaphthoyl}}$), 1.81–1.74 (m, 1H, 3b- $H_{\text{tetrahydronaphthoyl}}$). $^{13}\text{C-NMR}$ (151 MHz, $\text{DMSO-}d_6$, 299 K): δ (in ppm) = 175.6 (1 C, C=O), 158.1 (1 C, 5- $\text{C}_{\text{triazolyl}}$), 157.5 (1 C, 3- $\text{C}_{\text{triazolyl}}$), 145.7 (1 C, 5- $\text{C}_{\text{pyrazine}}$), 144.8 (1 C, 6- $\text{C}_{\text{pyrazine}}$), 144.6 (1 C, 2- $\text{C}_{\text{pyrazine}}$), 143.4 (1 C, 3- $\text{C}_{\text{pyrazine}}$), 137.5 (1 C, 4a- $\text{C}_{\text{tetrahydronaphthoyl}}$), 133.0 (1 C, 8a- $\text{C}_{\text{tetrahydronaphthoyl}}$), 129.4 (1 C, 8- $\text{C}_{\text{tetrahydronaphthoyl}}$), 129.2 (1 C, 5- $\text{C}_{\text{tetrahydronaphthoyl}}$), 126.8 (1 C, 6-/7- $\text{C}_{\text{tetrahydronaphthoyl}}$), 125.8 (1 C, 6-/7- $\text{C}_{\text{tetrahydronaphthoyl}}$), 43.3 (1 C, 1- $\text{C}_{\text{tetrahydronaphthoyl}}$), 28.6 (1 C, 4- $\text{C}_{\text{tetrahydronaphthoyl}}$), 26.3 (1 C, 2- $\text{C}_{\text{tetrahydronaphthoyl}}$), 19.9 (1 C, 3- $\text{C}_{\text{tetrahydronaphthoyl}}$). IR (neat): $\tilde{\nu}$ [cm^{-1}] = 3460, 3062, 2932, 1709, 1632, 1543, 1439, 1366, 1146, 1015, 741. HRMS (APCI): m/z = 321.1458 calculated for $\text{C}_{17}\text{H}_{17}\text{N}_6\text{O}^+$ [$\text{M}+\text{H}$] $^+$, found: 321.1457. HPLC: t_{R} = 19.0 min, purity: 96.1%.

(*S*)-(5-Amino-3-(2-methyl-6-(thiophen-2-yl)pyridin-3-yl)-1H-1,2,4-triazol-1-yl)(1,2,3,4-tetrahydro-naphthalen-1-yl)methanone (**33d**). Compound **29f** (80 mg, 311 μmol , 1.0 eq.), (*S*)-1,2,3,4-tetrahydronaphthalene-1-carboxylic acid (55 mg, 311 μmol , 1.0 eq.), DMAP (76 mg, 622 μmol , 2.0 eq.) and EDCI-HCl (119 mg, 622 μmol , 2.0 eq.) were dissolved in DMF (7 mL, dry) and pyridine (2 mL, dry) at 0°C under nitrogen atmosphere. The solution was stirred at 0°C for 1 h and then at r.t. for 4 h. The reaction mixture was poured into cold H_2O and stored at 4°C for 15 min. The formed precipitate was filtered off and washed with H_2O and Et_2O . The remaining solid was dried *in vacuo*, the product was obtained as a colourless solid (113 mg, 272 μmol , 87%). M.p. = 176.5°C. TLC: R_{f} = 0.38 (DCM/MeOH = 20/1). $^1\text{H-NMR}$ (600 MHz, $\text{DMSO-}d_6$, 299 K): δ (in ppm) = 8.31 (d, $J=8.2$ Hz, 1H, 4- H_{pyridyl}), 7.88 (d, $J=8.2$ Hz, 1H, 5- H_{pyridyl}), 7.85 (d, $J=3.7$ Hz, 1H, 3-/5- $H_{\text{thiophenyl}}$), 7.73 (s, 2H, - NH_2), 7.68 (d, $J=5.0$ Hz, 1H, 3-/5- $H_{\text{thiophenyl}}$), 7.19 (dd, $J=5.0, 3.7$ Hz, 1H, 4- $H_{\text{thiophenyl}}$), 7.18–7.14 (m, 2H, 5- $H_{\text{tetrahydronaphthoyl}}$ 6-/7- $H_{\text{tetrahydronaphthoyl}}$), 7.14–7.09 (m, 2H, 8- $H_{\text{tetrahydronaphthoyl}}$ 6-/7- $H_{\text{tetrahydronaphthoyl}}$), 5.02 (t, $J=6.3$ Hz, 1H, 1- $H_{\text{tetrahydronaphthoyl}}$), 2.84 (s, 3H, - CH_3), 2.83–2.73 (m, 2H, 4- $H_{\text{tetrahydronaphthoyl}}$), 2.25–2.14 (m, 2H, 2- $H_{\text{tetrahydronaphthoyl}}$), 1.94–1.86 (m, 1H, 3a- $H_{\text{tetrahydronaphthoyl}}$), 1.81–1.73 (m, 1H, 3b- $H_{\text{tetrahydronaphthoyl}}$). $^{13}\text{C-NMR}$ (151 MHz, $\text{DMSO-}d_6$, 299 K): δ (in ppm) = 175.4 (1 C, C=O), 158.7 (1 C, 3- $\text{C}_{\text{triazolyl}}$), 157.3 (1 C, 5- $\text{C}_{\text{triazolyl}}$), 156.5 (1 C, 2- $\text{C}_{\text{pyridyl}}$), 151.4 (1 C, 6- $\text{C}_{\text{pyridyl}}$), 144.0 (1 C, 2- $\text{C}_{\text{thiophenyl}}$), 137.7 (1 C, 4- $\text{C}_{\text{pyridyl}}$), 137.5 (1 C, 4a- $\text{C}_{\text{tetrahydronaphthoyl}}$), 133.1 (1 C, 8a- $\text{C}_{\text{tetrahydronaphthoyl}}$), 129.3 (1 C, 8- $\text{C}_{\text{tetrahydronaphthoyl}}$), 129.2 (1 C, 5- $\text{C}_{\text{tetrahydronaphthoyl}}$), 129.1 (1 C, 3-/5- $\text{C}_{\text{thiophenyl}}$), 128.5 (1 C, 4- $\text{C}_{\text{thiophenyl}}$), 126.8 (1 C, 6-/7- $\text{C}_{\text{tetrahydronaphthoyl}}$), 125.9 (1 C, 3-/5- $\text{C}_{\text{thiophenyl}}$), 125.8 (1 C, 6-/7- $\text{C}_{\text{tetrahydronaphthoyl}}$), 122.9 (1 C, 3- $\text{C}_{\text{pyridyl}}$), 116.0 (5- $\text{C}_{\text{pyridyl}}$), 43.7 (1 C, 1- $\text{C}_{\text{tetrahydronaphthoyl}}$), 28.6 (1 C, 4- $\text{C}_{\text{tetrahydronaphthoyl}}$), 26.2 (1 C, 2- $\text{C}_{\text{tetrahydronaphthoyl}}$), 25.2 (1 C, - CH_3), 20.1 (1 C, 3- $\text{C}_{\text{tetrahydronaphthoyl}}$). IR (neat): $\tilde{\nu}$ [cm^{-1}] = 3453, 3017, 2932, 1709, 1647, 1574, 1466, 1369, 1319, 1153, 991, 745. HRMS (APCI): m/z = 416.1540 calculated for $\text{C}_{23}\text{H}_{22}\text{N}_5\text{OS}^+$ [$\text{M}+\text{H}$] $^+$, found: 416.1579. HPLC: t_{R} = 22.7 min, purity: 95.3%.

(*S*)-(5-Amino-3-(tert-butyl)-1H-1,2,4-triazol-1-yl)(1,2,3,4-tetrahydro-naphthalen-1-yl)methanone (**33e**). Compound **15h** (80 mg, 571 μmol , 1.0 eq.), (*S*)-1,2,3,4-tetrahydronaphthalene-1-carboxylic acid (101 mg, 571 μmol , 1.0 eq.), DMAP (139 mg, 1.14 mmol, 2.0 eq.) and EDCI-HCl (219 mg, 1.14 mmol, 2.0 eq.) were dissolved in DMF (7 mL, dry), and pyridine (2 mL, dry) at 0°C under nitrogen atmosphere. The solution was stirred at 0°C for 1 h and then at r.t. for 4 h. The reaction mixture was poured into cold H_2O and stored at 4°C for 15 min. The formed precipitate was filtered off and washed with H_2O and Et_2O . The remaining solid was dried *in vacuo*, the product was obtained as a colourless solid (143 mg, 481 μmol , 84%). M.p. = 132.5°C. TLC: R_{f} = 0.43 (DCM/MeOH = 20/1). $^1\text{H-NMR}$ (600 MHz, $\text{DMSO-}d_6$, 299 K): δ (in ppm) = 7.47 (s, 2H, - NH_2), 7.17–7.11 (m, 2H, 8- $H_{\text{tetrahydronaphthoyl}}$ 6-/7- $H_{\text{tetrahydronaphthoyl}}$), 7.08 (dd, $J=8.6, 6.8$ Hz, 1H, 6-/7- $H_{\text{tetrahydronaphthoyl}}$), 7.03 (d, $J=8.4$ Hz, 1H, 5- $H_{\text{tetrahydronaphthoyl}}$), 4.90 (t, $J=6.4$ Hz, 1H, 1- $H_{\text{tetrahydronaphthoyl}}$), 2.84–2.69 (m,

2H, 4- $H_{\text{tetrahydronaphthoyl}}$), 2.14–2.03 (m, 2H, 2- $H_{\text{tetrahydronaphthoyl}}$), 1.92–1.84 (m, 1H, 3a- $H_{\text{tetrahydronaphthoyl}}$), 1.78–1.67 (m, 1H, 3b- $H_{\text{tetrahydronaphthoyl}}$), 1.27 (s, 9H, - $\text{C}(\text{CH}_3)_3$). $^{13}\text{C-NMR}$ (151 MHz, $\text{DMSO-}d_6$, 299 K): δ (in ppm) = 175.3 (1 C, C=O), 170.2 (1 C, 3- $\text{C}_{\text{triazolyl}}$), 157.5 (1 C, 5- $\text{C}_{\text{triazolyl}}$), 137.5 (1 C, 4a- $\text{C}_{\text{tetrahydronaphthoyl}}$), 133.2 (1 C, 8a- $\text{C}_{\text{tetrahydronaphthoyl}}$), 129.1 (1 C, 8- $\text{C}_{\text{tetrahydronaphthoyl}}$), 129.1 (1 C, 5- $\text{C}_{\text{tetrahydronaphthoyl}}$), 126.7 (1 C, 6-/7- $\text{C}_{\text{tetrahydronaphthoyl}}$), 125.7 (1 C, 6-/7- $\text{C}_{\text{tetrahydronaphthoyl}}$), 43.2 (1 C, 1- $\text{C}_{\text{tetrahydronaphthoyl}}$), 32.5 (1 C, - $\text{C}(\text{CH}_3)_3$), 28.6 (3 C, - $\text{C}(\text{CH}_3)_3$), 26.1 (1 C, 3a- $\text{C}_{\text{tetrahydronaphthoyl}}$), 20.0 (1 C, 3b- $\text{C}_{\text{tetrahydronaphthoyl}}$). IR (neat): $\tilde{\nu}$ [cm^{-1}] = 3433, 3020, 2970, 1709, 1643, 1543, 1450, 1373, 1273, 1196, 991, 745. HRMS (APCI): m/z = 299.1866 calculated for $\text{C}_{17}\text{H}_{23}\text{N}_4\text{O}^+$ [$\text{M}+\text{H}$] $^+$, found: 299.1863. HPLC: t_{R} = 20.8 min, purity: 96.2%.

(*S*)-(5-Amino-3-(4-fluorophenyl)-1H-1,2,4-triazol-1-yl)(1,2,3,4-tetrahydro-naphthalen-1-yl)-methanone (**33f**). Compound **15i** (80 mg, 449 μmol , 1.0 eq.), (*S*)-1,2,3,4-tetrahydronaphthalene-1-carboxylic acid (79 mg, 449 μmol , 1.0 eq.), DMAP (110 mg, 898 μmol , 2.0 eq.) and EDCI-HCl (172 mg, 898 μmol , 2.0 eq.) were dissolved in DMF (7 mL, dry) and pyridine (2 mL, dry) at 0°C under nitrogen atmosphere. The solution was stirred at 0°C for 1 h and then at r.t. for 4 h. The reaction mixture was poured into cold H_2O and stored at 4°C for 15 min. The formed precipitate was filtered off and washed thoroughly with H_2O . The remaining solid was dried *in vacuo*, the product was obtained as a colourless solid (140 mg, 416 μmol , 93%). M.p. = 204.5°C. TLC: R_{f} = 0.49 (DCM/MeOH = 20/1). $^1\text{H-NMR}$ (600 MHz, $\text{DMSO-}d_6$, 299 K): δ (in ppm) = 8.08–8.02 (m, 2H, 2-/6- $H_{\text{fluorophenyl}}$), 7.72 (s, 2H, - NH_2), 7.35–7.30 (m, 2H, 3-/5- $H_{\text{fluorophenyl}}$), 7.20–7.13 (m, 2H, 5- $H_{\text{tetrahydronaphthoyl}}$ 6-/7- $H_{\text{tetrahydronaphthoyl}}$), 7.12–7.06 (m, 2H, 8- $H_{\text{tetrahydronaphthoyl}}$ 6-/7- $H_{\text{tetrahydronaphthoyl}}$), 5.04 (t, $J=6.4$ Hz, 1H, 1- $H_{\text{tetrahydronaphthoyl}}$), 2.85–2.74 (m, 2H, 4- $H_{\text{tetrahydronaphthoyl}}$), 2.22–2.16 (m, 1H, 2a- $H_{\text{tetrahydronaphthoyl}}$), 2.15–2.08 (m, 1H, 2b- $H_{\text{tetrahydronaphthoyl}}$), 1.94–1.86 (m, 1H, 3a- $H_{\text{tetrahydronaphthoyl}}$), 1.80–1.72 (m, 1H, 3b- $H_{\text{tetrahydronaphthoyl}}$). $^{13}\text{C-NMR}$ (151 MHz, $\text{DMSO-}d_6$, 299 K): δ (in ppm) = 175.4 (1 C, C=O), 163.3 (d, $J_{\text{C,F}}$ = 247.4 Hz, 1 C, 4- $\text{C}_{\text{fluorophenyl}}$), 158.8 (1 C, 3- $\text{C}_{\text{triazolyl}}$), 158.0 (1 C, 5- $\text{C}_{\text{triazolyl}}$), 137.5 (1 C, 4a- $\text{C}_{\text{tetrahydronaphthoyl}}$), 133.1 (1 C, 8a- $\text{C}_{\text{tetrahydronaphthoyl}}$), 129.3 (1 C, 8- $\text{C}_{\text{tetrahydronaphthoyl}}$), 129.2 (1 C, 5- $\text{C}_{\text{tetrahydronaphthoyl}}$), 128.8 (d, $J_{\text{C,F}}$ = 8.7 Hz, 2 C, 2-/6- $\text{C}_{\text{fluorophenyl}}$), 126.8 (1 C, 6-/7- $\text{C}_{\text{tetrahydronaphthoyl}}$), 126.7 (d, $J_{\text{C,F}}$ = 2.9 Hz, 1 C, 1- $\text{C}_{\text{fluorophenyl}}$), 125.8 (1 C, 6-/7- $\text{C}_{\text{tetrahydronaphthoyl}}$), 115.8 (d, $J_{\text{C,F}}$ = 22.0 Hz, 2 C, 3-/5- $\text{C}_{\text{fluorophenyl}}$), 43.3 (1 C, 1- $\text{C}_{\text{tetrahydronaphthoyl}}$), 28.6 (1 C, 4- $\text{C}_{\text{tetrahydronaphthoyl}}$), 26.2 (1 C, 2- $\text{C}_{\text{tetrahydronaphthoyl}}$), 20.0 (1 C, 3- $\text{C}_{\text{tetrahydronaphthoyl}}$). IR (neat): $\tilde{\nu}$ [cm^{-1}] = 3426, 3024, 2924, 1717, 1643, 1543, 1126, 991, 841, 741, 610. HRMS (APCI): m/z = 337.1459 calculated for $\text{C}_{19}\text{H}_{18}\text{FN}_4\text{O}^+$ [$\text{M}+\text{H}$] $^+$, found: 337.1459. HPLC: t_{R} = 22.4 min, purity: 98.3%.

(*S*)-(5-Amino-3-(quinolin-2-yl)-1H-1,2,4-triazol-1-yl)(1,2,3,4-tetrahydro-naphthalen-1-yl)-methanone (**33g**). Compound **15k** (100 mg, 473 μmol , 1.0 eq.), (*S*)-1,2,3,4-tetrahydronaphthalene-1-carboxylic acid (83 mg, 473 μmol , 1.0 eq.), DMAP (116 mg, 947 μmol , 2.0 eq.) and EDCI-HCl (182 mg, 947 μmol , 2.0 eq.) were dissolved in DMF (7 mL) and pyridine (2 mL, both dry) under nitrogen atmosphere at 0°C. The solution was stirred at 0°C for 1 h and then at r.t. for 4 h. The reaction mixture was poured into cold H_2O and stored at 4°C for 15 min. The formed precipitate was washed thoroughly with H_2O , the remaining product was dried *in vacuo*. The product was obtained as a slight brown solid (80 mg, 216 μmol , 44%). M.p. = 206.5°C. TLC: R_{f} = 0.48 (DCM/MeOH = 20/1). $^1\text{H-NMR}$ (600 MHz, $\text{DMSO-}d_6$, 299 K): δ (in ppm) = 8.51 (d, $J=8.5$ Hz, 1H, 4- $H_{\text{quinoline}}$), 8.22 (d, $J=8.5$ Hz, 1H, 3- $H_{\text{quinoline}}$), 8.13 (d, $J=8.4$ Hz, 1H, 8- $H_{\text{quinoline}}$), 8.05 (d, $J=8.0$ Hz, 1H, 5- $H_{\text{quinoline}}$), 7.83 (t, $J=8.4, 7.4$ Hz, 1H, 7- $H_{\text{quinoline}}$), 7.78 (s, 2H, - NH_2), 7.67 (d, $J=7.4, 8.0$ Hz, 1H, 6- $H_{\text{quinoline}}$), 7.21–7.15 (m, 2H, 5-/8- $H_{\text{tetrahydronaphthoyl}}$), 7.15–7.06 (m, 2H, 6-/7- $H_{\text{tetrahydronaphthoyl}}$), 5.14 (t, $J=6.4$ Hz, 1H, 1- $H_{\text{tetrahydronaphthoyl}}$), 2.89–2.74 (m, 2H, 4- $H_{\text{tetrahydronaphthoyl}}$), 2.28–2.20 (m, 1H, 2a- $H_{\text{tetrahydronaphthoyl}}$), 2.18–2.10 (m, 1H, 2b- $H_{\text{tetrahydronaphthoyl}}$), 1.99–1.87 (m, 1H, 3a- $H_{\text{tetrahydronaphthoyl}}$), 1.86–1.75 (m, 1H, 3b- $H_{\text{tetrahydronaphthoyl}}$). $^{13}\text{C-NMR}$ (151 MHz, $\text{DMSO-}d_6$, 299 K): δ (in ppm) = 175.8 (1 C, C=O), 159.7 (1 C, 3- $\text{C}_{\text{triazolyl}}$), 157.4 (1 C, 3-

C-triazolyl), 149.1 (1 C, 2-*C*-quinoline), 147.4 (1 C, 8a-*C*-quinoline), 137.5 (1 C, 4a-*C*-tetrahydronaphthoyl), 137.0 (1 C, 4-*C*-quinoline), 133.1 (1 C, 8a-*C*-tetrahydronaphthoyl), 130.2 (1 C, 7-*C*-quinoline), 129.3 (1 C, 8-*C*-quinoline), 129.3 (1 C, 8-*C*-tetrahydronaphthoyl), 129.2 (1 C, 5-*C*-tetrahydronaphthoyl), 128.0 (1 C, 5-*C*-quinoline), 128.0 (1 C, 4a-*C*-quinoline), 127.4 (1 C, 6-*C*-quinoline), 126.8 (1 C, 6-/7-*C*-tetrahydronaphthoyl), 125.8 (1 C, 6-/7-*C*-tetrahydronaphthoyl), 120.0 (1 C, 3-*C*-quinoline), 43.3 (1 C, 1-*C*-tetrahydronaphthoyl), 28.6 (1 C, 4-*C*-tetrahydronaphthoyl), 25.9 (1 C, 2-*C*-tetrahydronaphthoyl), 20.0 (1 C, 3-*C*-tetrahydronaphthoyl). IR (neat): ν [cm⁻¹] = 3468, 3062, 2932, 1708, 1635, 1528, 1400, 1369, 1157, 991, 833, 763. HRMS (APCI): m/z = 370.1662 calculated for C₂₂H₂₀N₅O⁺ [M + H]⁺, found: 370.1663. HPLC: t_R = 20.7 min, purity: 95.9%.

(*S*)-(5-Amino-3-(3-methylquinoxalin-2-yl)-1H-1,2,4-triazol-1-yl)(1,2,3,4-tetrahydronaphthalen-1-yl)methanone (**33h**). Compound **24a** (40 mg, 177 μmol, 1.0 eq.), (*S*)-1,2,3,4-tetrahydronaphthalene-1-carboxylic acid (31 mg, 177 μmol, 1.0 eq.), DMAP (43 mg, 354 μmol, 2.0 eq.) and EDCI·HCl (68 mg, 354 μmol, 2.0 eq.) were dissolved in DMF (4 mL, dry) and pyridine (1 mL, dry) under nitrogen atmosphere at 0 °C. The solution was stirred at 0 °C for 1 h and then at r.t. for 4 h. The reaction mixture was poured into cold H₂O and stored at 4 °C for 15 min. The formed precipitate was filtered off and washed with H₂O and Et₂O. The remaining product was dried *in vacuo* and was obtained as a colourless solid (22 mg, 57 μmol, 32%). M.p. = 206.5 °C. TLC: R_f = 0.48 (DCM/MeOH = 20/1). ¹H-NMR (600 MHz, DMSO-*d*₆, 299 K): δ (in ppm) = 8.14 (d, J = 8.2 Hz, 1H, 5-/8-*H*-quinoline), 8.07 (d, J = 8.2 Hz, 1H, 5-/8-*H*-quinoline), 7.89 (dd, J = 8.2, 6.9 Hz, 1H, 6-/7-*H*-quinoline), 7.85 (dd, J = 8.2, 6.9 Hz, 1H, 6-/7-*H*-quinoline), 7.79 (s, 2H, -NH₂), 7.20–7.09 (m, 4H, 5-/6-/7-8-*H*-tetrahydronaphthoyl), 5.05 (t, J = 6.3 Hz, 1H, 1-*H*-tetrahydronaphthoyl), 2.98 (s, 3H, -CH₃), 2.90–2.68 (m, 2H, 4-*H*-tetrahydronaphthoyl), 2.27–2.14 (m, 2H, 2-*H*-tetrahydronaphthoyl), 1.95–1.85 (m, 1H, 3a-*H*-tetrahydronaphthoyl), 1.83–1.74 (m, 1H, 3b-*H*-tetrahydronaphthoyl). ¹³C-NMR (151 MHz, DMSO-*d*₆, 299 K): δ (in ppm) = 175.6 (1 C, C=O), 158.9 (1 C, 3-/5-*C*-triazolyl), 157.6 (1 C, 3-/5-*C*-triazolyl), 153.2 (1 C, 2-*C*-quinoxaline), 144.4 (1 C, 3-*C*-quinoxaline), 140.9 (1 C, 4a-/8a-*C*-quinoxaline), 139.9 (1 C, 4a-/8a-*C*-quinoxaline), 137.5 (1 C, 4a-*C*-tetrahydronaphthoyl), 133.0 (1 C, 8a-*C*-tetrahydronaphthoyl), 131.1 (1 C, 6-/7-*C*-quinoxaline), 129.8 (1 C, 6-/7-*C*-quinoxaline), 129.4 (1 C, 8-*C*-tetrahydronaphthoyl), 129.2 (1 C, 5-*C*-tetrahydronaphthoyl), 129.1 (1 C, 5-/8-*C*-quinoxaline), 128.2 (1 C, 5-/8-*C*-quinoxaline), 126.9 (1 C, 6-/7-*C*-tetrahydronaphthoyl), 125.8 (1 C, 6-/7-*C*-tetrahydronaphthoyl), 43.7 (1 C, 1-*C*-tetrahydronaphthoyl), 28.6 (1 C, 4-*C*-tetrahydronaphthoyl), 26.3 (1 C, 2-*C*-tetrahydronaphthoyl), 24.5 (1 C, -CH₃), 20.0 (1 C, 3-*C*-tetrahydronaphthoyl). IR (neat): ν [cm⁻¹] = 3464, 3051, 2936, 1713, 1636, 1558, 1369, 1138, 1099, 988, 752. HRMS (APCI): m/z = 385.1771 calculated for C₂₂H₂₁N₅O⁺ [M + H]⁺, found: 385.1774. HPLC: t_R = 21.2 min, purity: 95.9%.

(*S*)-(5-Amino-3-(isoquinolin-1-yl)-1H-1,2,4-triazol-1-yl)(1,2,3,4-tetrahydronaphthalen-1-yl)methanone (**33i**). Compound **15u** (70 mg, 331 μmol, 1.0 eq.), (*S*)-1,2,3,4-tetrahydronaphthalene-1-carboxylic acid (58 mg, 331 μmol, 1.0 eq.), DMAP (81 mg, 663 μmol, 2.0 eq.) and EDCI·HCl (127 mg, 663 μmol, 2.0 eq.) were dissolved in DMF (7 mL, dry) and pyridine (2 mL, dry) at 0 °C under nitrogen atmosphere. The solution was stirred at 0 °C for 1 h and then at r.t. for 4 h. The reaction mixture was poured into cold H₂O and stored at 4 °C for 15 min. The formed precipitate was filtered off and washed with H₂O and Et₂O. The remaining solid was dried *in vacuo*, the product was obtained as a slightly brown solid (70 mg, 189 μmol, 57%). M.p. = 192.5 °C. TLC: R_f = 0.32 (DCM/MeOH = 20/1). ¹H-NMR (600 MHz, DMSO-*d*₆, 299 K): δ (in ppm) = 8.83 (d, J = 8.6 Hz, 1H, 8-*H*-isoquinoline), 8.63 (d, J = 5.6 Hz, 1H, 3-*H*-isoquinoline), 8.06 (d, J = 8.2 Hz, 1H, 5-*H*-isoquinoline), 7.98 (d, J = 5.6 Hz, 1H, 4-*H*-isoquinoline), 7.85–7.77 (m, 3H, 6-*H*-isoquinoline -NH₂), 7.71 (dd, J = 8.6, 7.7 Hz, 1H, 7-*H*-isoquinoline), 7.22–7.09 (m, 4H, 5-/6-/7-/8-*H*-tetrahydronaphthoyl), 5.03 (t, J = 6.4 Hz, 1H, 1-*H*-tetrahydronaphthoyl), 2.86–2.74 (m, 2H, 4-*H*-tetrahydronaphthoyl), 2.27–2.12 (m, 2H, 2-*H*-tetrahydronaphthoyl), 1.96–1.87 (m, 1H, 3a-*H*-tetrahydronaphthoyl), 1.82–1.75 (m, 1H, 3b-*H*-tetrahydronaphthoyl). ¹³C-NMR (151 MHz, DMSO-*d*₆, 299 K): δ (in ppm) = 175.7 (1 C, C=O), 159.7 (1 C, 3-/5-*C*-triazolyl), 157.5 (1 C, 3-/5-*C*-triazolyl), 149.3 (1 C, 1-*C*-isoquinoline), 141.6 (1 C, 3-*C*-isoquinoline), 137.5 (1 C,

4a-*C*-tetrahydronaphthoyl), 136.3 (1 C, 4a-*C*-isoquinoline), 133.1 (1 C, 8a-*C*-tetrahydronaphthoyl), 130.5 (1 C, 6-*C*-isoquinoline), 129.3 (1 C, 5-/6-/7-/8-*C*-tetrahydronaphthoyl), 129.2 (1 C, 5-/6-/7-/8-*C*-tetrahydronaphthoyl), 128.1 (1 C, 7-*C*-isoquinoline), 127.2 (1 C, 5-*C*-isoquinoline), 126.9 (1 C, 8-*C*-isoquinoline), 126.8 (1 C, 5-/6-/7-/8-*C*-tetrahydronaphthoyl), 126.5 (1 C, 8a-*C*-isoquinoline), 125.8 (1 C, 5-/6-/7-/8-*C*-tetrahydronaphthoyl), 122.1 (1 C, 4-*C*-isoquinoline), 43.8 (1 C, 1-*C*-tetrahydronaphthoyl), 28.6 (1 C, 4-*C*-tetrahydronaphthoyl), 26.3 (1 C, 2-*C*-tetrahydronaphthoyl), 20.0 (1 C, 3-*C*-tetrahydronaphthoyl). IR (neat): ν [cm⁻¹] = 3468, 3048, 2940, 1705, 1639, 1520, 1369, 1153, 1092, 822, 756, 648. HRMS (APCI): m/z = 370.1662 calculated for C₂₂H₂₀N₅O⁺ [M + H]⁺, found: 370.1612. HPLC: t_R = 20.2 min, purity: 95.3%.

(*S*)-(2-(5-Amino-1-(1,2,3,4-tetrahydronaphthalen-1-carbonyl)-1H-1,2,4-triazol-3-yl)phenyl)(piperidin-1-yl)methanone (**33j**). (2-(5-amino-1H-1,2,4-triazol-3-yl)phenyl)(piperidin-1-yl)-methanone (80 mg, 295 μmol, 1.0 eq.), (*S*)-1,2,3,4-tetrahydronaphthalene-1-carboxylic acid (52 mg, 295 μmol, 1.0 eq.), DMAP (72 mg, 590 μmol, 2.0 eq.) and EDCI·HCl (113 mg, 590 μmol, 2.0 eq.) were dissolved in DMF (7 mL, dry) and pyridine (2 mL, dry) at 0 °C under nitrogen atmosphere. The solution was stirred at 0 °C for 1 h and then at r.t. for 4 h. The reaction mixture was poured into cold H₂O and stored at 4 °C for 15 min. The formed precipitate was filtered off and washed with H₂O and Et₂O. The remaining solid was dried *in vacuo*, the product was obtained as a colourless solid (61.6 mg, 143 μmol, 49%). M.p. = 166 °C. TLC: R_f = 0.39 (DCM/MeOH = 20/1). ¹H-NMR (600 MHz, DMSO-*d*₆, 299 K): δ (in ppm) = 8.02–7.96 (m, 1H, 3-*H*-phenyl), 7.68 (s, 2H, -NH₂), 7.54–7.50 (m, 2H, 4-/5-*H*-phenyl), 7.30–7.26 (m, 1H, 6-*H*-phenyl), 7.21–7.13 (m, 2H, 5-/6-/7-*H*-tetrahydronaphthoyl), 7.13–7.07 (m, 1H, 6-/7-/8-*H*-tetrahydronaphthoyl), 7.06–7.00 (m, 1H, 6-/7-/8-*H*-tetrahydronaphthoyl), 4.97* (t, J = 6.3 Hz, 0.45H, 1-*H*-tetrahydronaphthoyl), 4.91 (t, J = 6.5 Hz, 0.55H, 1-*H*-tetrahydronaphthoyl), 4.01–3.85 (m, 1H, 2-/6-*H*-piperidyl), 3.20–2.93 (m, 3H, 2-/6-*H*-piperidyl), 2.86–2.72 (m, 2H, 4-*H*-tetrahydronaphthoyl), 2.19–2.00 (m, 2H, 2-*H*-tetrahydronaphthoyl), 1.99–1.67 (m, 2H, 3-*H*-tetrahydronaphthoyl), 1.66–1.58 (m, 1H, 3-/4-/5-*H*-piperidyl), 1.57–1.50 (m, 1H, 3-/4-/5-*H*-piperidyl), 1.47–1.38 (m, 2H, 3-/4-/5-*H*-piperidyl), 1.37–1.28 (m, 2H, 3-/4-/5-*H*-piperidyl). ¹³C-NMR (151 MHz, DMSO-*d*₆, 299 K): δ (in ppm) = 175.4* (1 C, C=O-tetrahydronaphthoyl), 168.4 (1 C, C=O-piperidyl/phenyl), 158.8* (1 C, 3-*C*-triazolyl), 157.5* (1 C, 5-*C*-triazolyl), 137.5 (1 C, 4a-*C*-tetrahydronaphthoyl), 136.5* (1 C, 1-*C*-phenyl), 133.1* (1 C, 8a-*C*-tetrahydronaphthoyl), 130.1 (2 C, 4-/5-*C*-phenyl), 129.3* (1 C, 5-*C*-tetrahydronaphthoyl), 129.2* (1 C, 6-/7-/8-*C*-tetrahydronaphthoyl), 128.7* (1 C, 3-*C*-phenyl), 128.5 (1 C, 2-*C*-phenyl), 126.9* (1 C, 6-/7-/8-*C*-tetrahydronaphthoyl), 126.8* (1 C, 6-*C*-phenyl), 126.7* (1 C, 2-*C*-phenyl), 125.9* (1 C, 6-/7-/8-*C*-tetrahydronaphthoyl), 47.1* (1 C, 2-/6-*C*-piperidyl), 43.6* (1 C, 1-*C*-tetrahydronaphthoyl), 41.5* (1 C, 2-/6-*C*-piperidyl), 28.6* (1 C, 4-*C*-tetrahydronaphthoyl), 26.4 (1 C, 2-*C*-tetrahydronaphthoyl), 25.2* (1 C, 4-*C*-piperidyl), 24.9* (1 C, 3-/5-*C*-piperidyl), 24.0* (1 C, 3-/5-*C*-piperidyl), 20.2* (1 C, 3-*C*-piperidyl), *— two rotamers exist in the ratio **33j**/**33j*** = 1.2/1, signals of the minor rotamer **33j*** are marked with *. IR (neat): ν [cm⁻¹] = 3422, 3024, 2936, 1709, 1635, 1601, 1539, 1447, 1366, 1258, 991, 741. HRMS (APCI): m/z = 430.2238 calculated for C₂₅H₂₈N₅O₂⁺ [M + H]⁺, found: 430.2237. HPLC: t_R = 21.1 min, 95.7%.

(*S*)-(5-Amino-3-(quinoxalin-2-yl)-1H-1,2,4-triazol-1-yl)(1,2,3,4-tetrahydronaphthalen-1-yl)methanone (**39a**). Compound **38** (81 mg, 0.38 mmol, 1.0 eq.) was suspended in DMF (7 mL, dry) and pyridine (2 mL, dry) and cooled down to 0 °C. (*S*)-1,2,3,4-Tetrahydronaphthalene-1-carboxylic acid (67 mg, 0.38 mmol, 1.0 eq.), EDCI·HCl (146 mg, 0.76 mmol, 2.0 eq.) and DMAP (93 mg, 0.76 mmol, 2.0 eq.) were added. The reaction mixture was stirred at 0 °C for 1 h and at r.t. for 3 h. The reaction mixture was poured into cold H₂O (100 mL) to precipitate the product. The precipitate was filtered off and washed vigorously with H₂O. The resulting pale red solid was dried *in vacuo*, no further purification was necessary (96.3 mg, 0.26 mmol, 68%). M.p. = 295 °C (decomp.). TLC: R_f = 0.33 (DCM/MeOH = 95/5). ¹H-NMR (600 MHz, DMSO-*d*₆, 299 K): δ (in ppm) = 9.55 (s, 1H, 3-*H*-quinoxaline), 8.24–8.20 (m, 1H, 8-*H*-quinoxaline), 8.19–8.15 (m, 1H, 5-*H*-quinoxaline), 8.00–7.91 (m, 2H, 6-/7-*H*-quinoxaline), 7.88 (s, 2H, -NH₂), 7.27–

7.04 (m, 4H, 5-/6-/7-/8-H_{quinoxaline}), 5.14 (t, $J=6.4$ Hz, 1H, 1-H_{tetrahydronaphthoyl}), 2.88–2.75 (m, 2H, 4-H_{quinoxaline}), 2.32–2.10 (m, 2H, 2-H_{quinoxaline}), 1.97–1.72 (m, 2H, 3-H_{quinoxaline}). ¹³C-NMR (151 MHz, DMSO-*d*₆, 299 K): δ (in ppm) = 175.7 (1 C, C=O), 158.2 (3-/5-C_{triazolyl}), 157.8 (1 C, 3-/5-C_{triazolyl}), 144.2 (1 C, 3-C_{quinoxaline}), 144.1 (1 C, 2-C_{quinoxaline}), 142.0 (1 C, 4a-C_{quinoxaline}), 141.3 (1 C, 8a-C_{quinoxaline}), 137.5 (1 C, 4a-C_{tetrahydronaphthoyl}), 133.0 (1 C, 8a-C_{tetrahydronaphthoyl}), 131.1 (1 C, 7-C_{quinoxaline}), 131.0 (1 C, 6-C_{quinoxaline}), 129.5 (1 C, 8-C_{quinoxaline}), 129.4 (1 C, 6-C_{tetrahydronaphthoyl}), 129.2 (1 C, 5-C_{tetrahydronaphthoyl}), 129.0 (1 C, 5-C_{quinoxaline}), 126.9 (1 C, 8-C_{tetrahydronaphthoyl}), 125.8 (1 C, 7-C_{tetrahydronaphthoyl}), 43.3 (1 C, 1-C_{tetrahydronaphthoyl}), 28.6 (1 C, 4-C_{tetrahydronaphthoyl}), 26.3 (1 C, 2-C_{tetrahydronaphthoyl}), 20.0 (1 C, 3-C_{tetrahydronaphthoyl}). IR (neat): $\tilde{\nu}$ [cm⁻¹] = 3464, 3271, 3176, 3065, 2928, 1711, 1639, 1520, 1495, 1460, 1366, 1301, 1256, 1244, 1163, 1113, 951, 745. HRMS (APCI): m/z = 361.1615 calculated for C₂₁H₁₉N₆O⁺ [M+H]⁺, found: 361.1609. HPLC: t_R = 20.8 min, purity: 97.2%.

(5-Amino-3-(quinoxalin-2-yl)-1H-1,2,4-triazol-1-yl)naphthalen-1-yl methanone (39b). Compound 38 (81 mg, 0.38 mmol, 1.0 eq.) was suspended in DMF (7 mL, dry) and pyridine (2 mL, dry), and the suspension was cooled down to 0 °C. 1-Naphtioic acid (68 mg, 0.38 mmol, 1.0 eq.), EDCI·HCl (146 mg, 0.76 mmol, 2.0 eq.) and DMAP (93 mg, 0.76 mmol, 2.0 eq.) were added, the mixture was stirred at 0 °C for 1 h and at r.t. for 3 h. The reaction mixture was poured into cold H₂O (100 mL), the resulting precipitation was filtered off and washed with H₂O and Et₂O. The product was dried *in vacuo* and obtained as a pale red solid (106 mg, 0.29 mmol, 76%), no further purification was necessary. M.p. = 280 °C (decomp.). TLC: R_f = 0.32 (DCM/MeOH = 95/5). ¹H-NMR (600 MHz, DMSO-*d*₆, 299 K): δ (in ppm) = 9.30 (s, 1H, 3-H_{quinoxaline}), 8.23 (d, J = 8.3 Hz, 1H, 4-H_{naphthoyl}), 8.14 (s, 2H, -NH₂), 8.12–8.08 (m, 3H, 5-/8-H_{quinoxaline}), 8.01 (d, J = 7.14 MHz, 1H, 2-H_{naphthoyl}), 8.00–7.96 (m, 1H, 8-H_{naphthoyl}), 7.91–7.85 (m, 2H, 6-/7-H_{quinoxaline}), 7.70 (dd, J = 8.3, 7.1 Hz, 1H, 3-H_{naphthoyl}), 7.66–7.60 (m, 2H, 6-/7-H_{naphthoyl}). ¹³C-NMR (151 MHz, DMSO-*d*₆, 299 K): δ (in ppm) = 169.0 (1 C, C=O), 158.9 (1 C, 3-/5-C_{triazolyl}), 158.0 (1 C, 3-/5-C_{triazolyl}), 144.1 (1 C, 3-C_{quinoxaline}), 144.0 (1 C, 2-C_{quinoxaline}), 141.9 (1 C, 4a-C_{quinoxaline}), 141.2 (1 C, 8a-C_{quinoxaline}), 132.9 (1 C, 1-C_{naphthoyl}), 131.7 (1 C, 4-C_{naphthoyl}), 131.0 (1 C, 6-/7-C_{quinoxaline}), 131.0 (1 C, 1-C_{naphthoyl}), 130.3 (1 C, 4a-C_{naphthoyl}), 129.5 (1 C, 5-/8-C_{quinoxaline}), 129.5 (1 C, 8a-C_{naphthoyl}), 129.0 (1 C, 5-/8-C_{naphthoyl}), 128.6 (1 C, 5-C_{naphthoyl}), 128.1 (1 C, 2-C_{naphthoyl}), 127.7 (1 C, 7-C_{naphthoyl}), 126.6 (1 C, 6-C_{naphthoyl}), 124.8 (1 C, 3-C_{naphthoyl}), 124.6 (1 C, 8-C_{naphthoyl}). IR (neat): $\tilde{\nu}$ [cm⁻¹] = 3462, 3267, 1686, 1639, 1518, 1456, 1366, 1271, 910, 802, 768, 741. HRMS (APCI): m/z = 367.1302 calculated for C₂₁H₁₅N₆O⁺ [M+H]⁺, found: 367.1300. HPLC: t_R = 20.0 min, purity: 98.7%.

(5-Amino-3-(quinoline-2-yl)-1H-1,2,4-triazol-1-yl)phenyl methanone (40a). Compound 15k (120.0 mg, 568 μ mol, 1.0 eq.) was dissolved in a mixture of pyridine (2 mL, dry) and THF (1 mL, dry), the solution was cooled down to 0 °C. Benzoyl chloride (79.9 mg, 568 μ mol, 1.0 eq.) in THF (1 mL, dry) was added dropwise (1 mL/h) under nitrogen atmosphere. The reaction mixture was stirred at 0 °C for 1 h, then warmed up to r.t. and stirred for another 1.5 h. The reaction was quenched by pouring the mixture into cold H₂O. The formed precipitate was filtered off and washed with a mixture of cyclohexane and Et₂O. The product was obtained as an amorphous colourless solid (156 mg, 495 μ mol, 87%). M.p. = 204 °C. TLC: R_f = 0.48 (DCM/MeOH = 95/5). ¹H-NMR (600 MHz, DMSO-*d*₆, 299 K): δ = (in ppm) 8.47 (d, J = 8.5 Hz, 1H, 3-H_{quinoxaline}), 8.16 (d, 2H, 2-/6-H_{phenyl}), 8.13 (d, J = 8.5 Hz, 1H, 4-H_{quinoxaline}), 8.09 (d, J = 8.4 Hz, 1H, 8-/5-H_{quinoxaline}), 8.02 (d, J = 6.7, 1H, 5-/8-H_{quinoxaline}), 7.90 (s, 2H, -NH₂), 7.81 (dd, J = 8.4, 6.7, 1H, 6-/7-H_{quinoxaline}), 7.72 (t, J = 7.4 Hz, 1H, 4-H_{phenyl}), 7.65 (dd, J = 7.5 Hz, 1H, 6-/7-H_{quinoxaline}), 7.62 (t, J = 7.4 Hz, 2H, 3-/5-H_{phenyl}). ¹³C-NMR (151 MHz, DMSO-*d*₆, 299 K) δ = 168.0 (1 C, C=O), 159.8 (1 C, 3-/5-C_{triazolyl}), 159.1 (1 C, 3-/5-C_{triazolyl}), 149.0 (1 C, 2-C_{quinoxaline}), 147.4 (1 C, 4a-/8a-C_{quinoxaline}), 136.9 (1 C, 3-C_{quinoxaline}), 133.1 (1 C, 4-

C_{phenyl}), 132.1 (1 C, 1-C_{phenyl}), 130.8 (1 C, 2-/6-C_{phenyl}), 130.1 (1 C, 6-/7-C_{quinoxaline}), 129.3 (1 C, 5-/8-C_{quinoxaline}), 128.2 (1 C, 3-/5-C_{quinoxaline}), 128.0 (1 C, 5-/8-C_{quinoxaline}), 127.9 (1 C, 4a-/8a-C_{quinoxaline}), 127.3 (1 C, 6-/7-C_{quinoxaline}), 119.8 (1 C, 4-C_{quinoxaline}). HRMS (APCI): m/z = 316.1193 calculated for C₁₆H₁₄N₅O⁺ [M+H]⁺, found: 316.1227. HPLC: t_R = 18.5 min, purity: 97.3%.

(5-Amino-3-(quinolin-2-yl)-1H-1,2,4-triazol-1-yl)naphthalen-1-yl methanone (40b). Compound 15k (102 mg, 482 μ mol, 1.0 eq.) was dissolved in the mixture of pyridine (3 mL, dry) and THF (2 mL, dry) and cooled down to 0 °C. Then, 1-naphtoylchloride (92 mg, 482 μ mol, 1.0 eq.) in THF (1 mL, dry) was added dropwise (1 mL/h) under nitrogen atmosphere. After stirring for 1 h at 0 °C and 1 h at r.t., More 1-naphtoylchloride (92 mg, 482 μ mol, 1.0 eq.) in THF (1 mL, dry) was added dropwise to the reaction. After 2 h stirring at r.t., the reaction was quenched by pouring the reaction mixture into cold H₂O. The formed precipitate was filtered off, washed with H₂O and EtOAc and dried *in vacuo*. The product could be obtained as a slightly yellowish solid (136 mg, 373 μ mol, 77%). M.p. = 205 °C. TLC: R_f = 0.37 (DCM/MeOH = 20/1). ¹H-NMR (600 MHz, DMSO-*d*₆, 299 K): δ (in ppm) = 8.39 (d, J = 8.7 Hz, 1H, 4-H_{quinoline}), 8.22 (d, J = 8.4 Hz, 1H, 2-H_{naphthoyl}), 8.12–8.08 (m, 1H, CH_{naphthoyl}), 8.03 (s, 2H, -NH₂), 8.01 (d, J = 8.5 Hz, 1H, 8-H_{quinoline}), 8.00–7.93 (m, 4H, 5-/3-H_{quinoline}), 4-/3-H_{naphthoyl}), 7.78–7.74 (m, 1H, 7-H_{quinoline}), 7.70 (dd, J = 8.2, 7.1 Hz, 1H, 3-H_{naphthoyl}), 7.65–7.59 (m, 3H, CH_{naphthoyl}). ¹³C-NMR (151 MHz, DMSO-*d*₆, 299 K): δ (in ppm) = 169.1 (1 C, C=O), 159.9 (1 C, 3-/5-C_{triazolyl}), 158.8 (1 C, 3-/5-C_{triazolyl}), 148.9 (1 C, 2-C_{quinoline}), 147.3 (1 C, 8a-C_{quinoline}), 136.9 (1 C, 4-C_{quinoline}), 132.9 (1 C, C_q), 131.5 (1 C, 2'-C_{naphthoyl}), 130.6 (1 C, C_q), 130.1 (1 C, 7-C_{quinoline}), 129.5 (1 C, C_q), 129.2 (1 C, 8-C_{quinoline}), 128.6 (1 C, CH_{naphthoyl}), 127.9 (2 C, 5-C_{quinoline}), 4-C_{naphthoyl}), 127.8 (1 C, C_q), 127.6 (1 C, CH_{naphthoyl}), 127.3 (1 C, CH_{naphthoyl}), 126.6 (1 C, CH_{naphthoyl}), 124.8 (1 C, 3-C_{naphthoyl}), 124.6 (1 C, CH_{naphthoyl}), 119.9 (1 C, 3-C_{quinoline}). IR (neat): $\tilde{\nu}$ [cm⁻¹] = 3464, 3048, 2326, 1686, 1639, 1508, 1366, 922, 829, 799, 763. HRMS (APCI): m/z = 366.1349 calculated for C₂₂H₁₆N₅O⁺ [M+H]⁺, found: 366.1321. HPLC: 19.9 min, purity: 96.7%.

(5-Amino-3-(isoquinolin-1-yl)-1H-1,2,4-triazol-1-yl)phenyl methanone (41a). Compound 15u (70 mg, 0.33 mmol) was dissolved in THF (6 mL, dry) and pyridine (2 mL, dry) under nitrogen atmosphere, the solution was cooled down to 0 °C. Benzoyl chloride (138 μ L, 1.20 mmol, 3.6 eq.) in THF (1 mL) added dropwise into the cold solution of 15u over 1 h. After complete addition, the reaction was heated to r.t. and stirred for additional 3 h. The reaction mixture was poured into cold H₂O, the forming precipitate was filtered off, washed with H₂O and dried *in vacuo*. After purification with flash chromatography, the product could be obtained as a colourless solid (104 mg, 0.33 mmol, > 99%). M.p. = 280 °C (decomp.). TLC: R_f = 0.41 (DCM/MeOH = 85/15). ¹H-NMR (400 MHz, DMSO-*d*₆, 299 K): δ (in ppm) = 8.79 (d, J = 8.6 Hz, 1H, 8-H_{isoquinoline}), 8.61 (d, J = 5.5 Hz, 1H, 3-H_{isoquinoline}), 8.17–8.11 (m, 2H, 2-/6-H_{benzoyl}), 8.05 (d, J = 8.2 Hz, 1H, 5-H_{isoquinoline}), 7.96 (d, J = 5.5 Hz, 1H, 4-H_{isoquinoline}), 7.92 (s, 2H, -NH₂), 7.81 (t, J = 8.2 Hz, 1H, 6-H_{isoquinoline}), 7.73–7.65 (m, 2H, 7-H_{isoquinoline}), 4-H_{benzoyl}), 7.60–7.55 (m, 2H, 3'-/5'-H_{benzoyl}). ¹³C-NMR (101 MHz, DMSO-*d*₆, 299 K): δ (in ppm) = 168.0 (1 C, C=O), 159.8 (1 C, 3-/5-C_{triazolyl}), 158.5 (3-/5-C_{triazolyl}), 149.3 (1 C, 1-C_{isoquinoline}), 142.0 (1 C, 3-C_{isoquinoline}), 136.2 (1 C, 4a-C_{isoquinoline}), 133.0 (1 C, 4-C_{benzoyl}), 132.1 (1 C, 1-C_{benzoyl}), 130.7 (2 C, 2-/5-C_{benzoyl}), 130.5 (1 C, 6-C_{benzoyl}), 128.1 (2 C, 3-/5-C_{benzoyl}), 128.0 (1 C, 7-C_{isoquinoline}), 127.1, (1 C, 5-C_{isoquinoline}) 126.8 (1 C, 8-C_{isoquinoline}), 126.5 (1 C, 8a-C_{isoquinoline}), 122.0 (1 C, 4-C_{isoquinoline}). IR (neat): $\tilde{\nu}$ [cm⁻¹] = 3470, 3028, 2980, 1688, 1643, 1520, 1447, 1267, 1152, 957, 789, 745, 719. HRMS (APCI): m/z = 316.1193 calculated for C₁₆H₁₄N₅O⁺ [M+H]⁺, found: 316.1192. HPLC: t_R = 17.4 min, purity: 96.3%.

(5-Amino-3-(isoquinolin-1-yl)-1H-1,2,4-triazol-1-yl)naphthalen-2-yl methanone (41c). Compound 15u (80 mg, 0.38 mmol) was suspended in DMF (7 mL) and pyridine (2 mL, both dry) under nitrogen

atmosphere. The mixture was cooled down to 0 °C and 2-naphthoic acid (65 mg, 0.38 mmol, 1.0 eq.), EDCI-HCl (145 mg, 0.76 mmol, 2.0 eq.) and DMAP (92 mg, 0.76 mmol, 2.0 eq.) were added. The reaction mixture was stirred at 0 °C for 1 h and at r.t. for 3 h. The reaction mixture was poured into cold H₂O, the forming precipitate was filtered off and washed with H₂O and Et₂O. After drying *in vacuo*, the product was obtained as a colourless solid (109 mg, 0.30 mmol, 79%). M.p. = 280 °C (decomp.). TLC: R_f = 0.32 (DCM/MeOH = 85/15). ¹H-NMR (600 MHz, DMSO-*d*₆, 299 K): δ (in ppm) = 8.89 (d, J = 8.6 Hz, 1H, 8-H_{isoquinoline}), 8.85 (s, 1H, 8-H_{naphthoyl}), 8.61 (d, J = 5.5 Hz, 1H, 3-H_{isoquinoline}), 8.17–8.11 (m, 2H, 2-/7-H_{naphthoyl}), 8.10–8.02 (m, 3H, 3-/4-H_{naphthoyl} 5-H_{isoquinoline}), 7.96 (d, J = 5.7 Hz, 1H, 4-H_{isoquinoline}), 7.95 (s, 2H, -NH₂), 7.82 (dd, J = 8.2, 6.7 Hz, 1H, 6-H_{isoquinoline}), 7.73–7.69 (m, 2H, 7-H_{isoquinoline} 5-H_{naphthoyl}), 7.65 (dd, J = 8.2, 6.8 Hz, 1H, 6-H_{naphthoyl}). ¹³C-NMR (151 MHz, DMSO-*d*₆, 299 K): δ (in ppm) = 168.0 (1 C, C=O), 159.8 (1 C, 3-/5-C_{triazolyl}), 158.5 (1 C, 3-/5-C_{triazolyl}), 149.2 (1 C, 1-C_{isoquinoline}), 142.0 (1 C, 3-C_{isoquinoline}), 136.2, (1 C, 4a-C_{isoquinoline}) 134.7 (1 C, 4a-C_{naphthoyl}), 132.3 (1 C, 8-C_{naphthoyl}), 131.6 (1 C, 7a-C_{naphthoyl}), 130.5 (1 C, 6-C_{isoquinoline}), 129.4 (1 C, 7-C_{isoquinoline}), 128.9 (1 C, 7-C_{naphthoyl}), 128.0 (1 C, 5-C_{naphthoyl}), 127.7 (1 C, 4-C_{naphthoyl}), 127.5 (1 C, 3-C_{naphthoyl}), 127.2 (1 C, 5-C_{isoquinoline}), 127.1 (1 C, 6-C_{naphthoyl}), 126.9 (1 C, 8-C_{naphthoyl}), 126.5 (1 C, 8a-C_{isoquinoline}), 126.2 (1 C, 2-C_{naphthoyl}), 122.1 (1 C, 4-C_{naphthoyl}). IR (neat): $\tilde{\nu}$ [cm⁻¹] = 3741, 3045, 1688, 1520, 1368, 1341, 1292, 1121, 1090, 922, 901, 854, 837. HRMS (APCI): m/z = 366.1350 calculated for C₂₂H₁₆N₅O⁺ [M+H]⁺, found: 366.1381. HPLC: t_R = 20.3 min, purity: 98.2%.

X-ray Diffraction. Data sets for compound **33 g** were collected with a Bruker D8 Venture PHOTON III diffractometer. Programs used: data collection: APEX3 V2019.1-0 (Bruker AXS Inc., Madison, Wisconsin, USA, 2019); cell refinement: SAINT V8.40 A (Bruker AXS Inc., Madison, Wisconsin, USA, 2019); data reduction: SAINT V8.40 A (Bruker AXS Inc., Madison, Wisconsin, USA, 2019); absorption correction, SADABS V2016/2 (Bruker AXS Inc., Madison, Wisconsin, USA, 2019); structure solution SHELXT-2015;^[21] structure refinement SHELXL-2015;^[22] and graphics, XP (Version 5.1, Bruker AXS Inc., Madison, Wisconsin, USA, 1998). R -values are given for observed reflections, and wR^2 values are given for all reflections. CCDC-12089066 (**33 g**) contains the supplementary crystallographic data for this paper. These data can be obtained free of charge from The Cambridge Crystallographic Data Centre via www.ccdc.cam.ac.uk/data_request/cif.

FXIIa Inhibition Assay. The inhibitory activity of synthesized compounds toward the human coagulation factor XIIa was measured by quantifying the hydrolysis rate of the fluorogenic substrate as reported previously.^[3f] Briefly, the activity was tested in buffer (10 mM Tris-Cl, 150 mM NaCl, 10 mM MgCl₂·6H₂O, 1 mM CaCl₂·2H₂O, 0.1% w/v BSA, 0.01% v/v Triton-X100, pH = 7.4) utilizing clear flat-bottom, black poly-styrene 96 well-plates. The enzyme (human β -FXIIa, HFXIIAB, >95% purity; Molecular Innovations, 2.5 nM final concentration) and the fluorogenic substrate Boc-Gln-Gly-Arg-AMC (Pepta Nova, 25 μ M final concentration, K_m = 167 μ M) were used. Dilutions of test-compounds ranging from 2 nM to 32 μ M (final concentrations) in DMSO were prepared. The fluorogenic substrate solution was added into the wells followed by the addition of 2 μ L of test-compounds solution, and the reaction was triggered by addition of the enzyme solution (final testing volume 152 μ L). In case of blank (substrate + buffer) and control (substrate + enzyme) wells, 2 μ L of DMSO was added instead of the test-compounds' solution. Fluorescence intensity was measured with Microplate Reader Mithras LB 940 (Berthold Technologies, excitation at 355 nm, emission at 460 nm) for a period of 1 h with a read every minute. The reactions were performed at 25 °C. To derive 1-hour IC₅₀ values, endpoint RFU (single fluorescence reading after 1 h) was used. Sigmoidal curves were prepared in GraphPad Prism software and IC₅₀ values were derived from the fitted curves.^[3f]

Thrombin Inhibition Assay. The inhibitory activity of synthesized compounds toward the coagulation factor IIa (human α -thrombin (active) protein, ABIN2127880, >95% purity; antibodies-online, 0.25 nM-final concentration) was determined analogously to the described procedure for FXIIa. The fluorogenic substrate Boc-Val-Pro-Arg-AMC (Pepta Nova, 25 μ M-final concentration, K_m = 18 μ M) was utilized.^[3f]

FXa Inhibition Assay. The inhibitory activity of synthesized compounds toward the coagulation factor Xa (human Factor Xa, HFXA, >95% purity; Molecular Innovations, 2.5 nM final concentration) was determined analogously to the described procedure for FXIIa. The fluorogenic substrate Boc-Ile-Glu-Gly-Arg-AMC (Pepta Nova, 25 μ M final concentration) was utilized.^[3f]

Trypsin Inhibition Assay. The inhibitory activity of synthesized compounds toward trypsin (porcine trypsin; Merck, 3.5 nM final concentration) was determined analogously to the described procedure for FXIIa. The fluorogenic substrate Z-Gly-Gly-Arg-AMC (Sigma-Aldrich, 25 μ M final concentration) was utilized.^[3f]

In Vitro Plasma Coagulation Assays (aPTT and PT). All measurements were performed using citrated (3.8%) human pooled plasma (Dunn Labortechnik GmbH, Germany) on a semi-automated coagulometer (Thrombotimer-2, Behnk Elektronik, Germany) according to the manufacturer instructions as previously reported.^[3f] For aPTT measurement, plasma (100 μ L) was placed into the incubation cuvettes of the instrument and incubated for 2 min at 37 °C. Then, test compound solution (10 μ L) or solvent (DMSO, 10 μ L) was added with a pipette. After 1 min of incubation, 100 μ L of prewarmed (37 °C) aPTT reagent (Convergent Technologies, Germany) was added and incubated for additional 2 min. The cuvettes were transferred to a measuring position, the coagulation was initiated by addition of 100 μ L of CaCl₂ solution (25 mM, prewarmed at 37 °C, Convergent Technologies, Germany) and the clotting time was recorded. For PT assays, plasma (100 μ L) was incubated for 2 min at 37 °C. Then, test compound solution (10 μ L) or solvent (DMSO, 10 μ L) was added with a pipette. After 3 min of incubation, the cuvettes were transferred to a measuring position, the coagulation was initiated by addition of 100 μ L of PT assay reagent already containing CaCl₂ (prewarmed at 37 °C, Convergent Technologies, Germany) and the clotting time was recorded.

Microscale Parallel Synthesis. 47 wells of 96-well plate (clear, polystyrene, flat bottom) were charged with (*S*)-1,2,3,4-tetrahydronaphthalene-1-carboxylic acid (**30**, 125 mmol/L in dry DMSO-*d*₆, 30 μ L, 1 equiv, each well) and other 47 wells with 2-iodophenylacetic acid (**31**, 125 mmol/L in dry DMSO-*d*₆, 30 μ L, 1 equiv, each well). Then a micro magnetic stirring bar was added in each well. EDCI-HCl (187.5 mmol/L in dry DMSO-*d*₆, 30 μ L, 1.5 equiv), DMAP (187.5 mmol/L in dry DMSO-*d*₆, 30 μ L, 1.5 equiv), and 47 different 1*H*-1,2,4-triazol-5-amines (125 mmol/L in dry DMSO-*d*₆, 30 μ L, 1 equiv) were sequentially pipetted into each well. The plate was covered with a lid, sealed with parafilm, and placed on the magnetic stirrer. After 3 h of incubation at room temperature, the lid was opened and 20 μ L aliquot from each microscale reaction was withdrawn, diluted with DMSO (980 μ L, dry) and immediately frozen at -20 °C (samples for MTS). The residual 100 μ L of the reaction solution were diluted with DMSO-*d*₆ (600 μ L, dry) and directly submitted for semi-q¹H-NMR analysis to measure the reaction conversion.

Determination of Microscale Reaction Conversions by semi-q¹H-NMR. The NMR spectra of microscale parallel synthesis samples were recorded at 25 °C using Agilent DD2 400 MHz NMR spectrometer and analyzed with MestReNova software (version 12.0.3-21384, Mestrelab Research S.L.). For (*S*)-1,2,3,4-tetrahydronaphthalene-1-carboxylic acid (**30**) amides (N-acylated products), the characteristic

proton resonance signal of the methine group (t , $J=6.3$ Hz, 1H, typically found between 4.60 and 5.10 ppm) was used for the calculations. For 2-iodophenylacetic acid (31) amides (N-acylated products), the characteristic proton resonance signal of the methylene bridge (s , 2H, typically found between 4.10 and 4.65 ppm) was used for the calculations. These proton signals of the product and the signals of the aromatic protons of DMAP (m , 2H, at 6.72 ppm or m , 2H, at 8.13 ppm) were identified, integrated, and normalized. The normalized integrals of the product protons (Int_p) and of DMAP (Int_R) were used to calculate the reactions' conversion (C,%) considering the used reaction equivalents (eq_R) according to the following formula: $C [\%] = (Int_p \times eq_R / Int_R) \times 100$. For the method development (Table 1), the purest proton resonance signals of the reaction product (13 a–e) and starting material (aminotriazole 7 or a carboxylic acid) were identified, integrated, and normalized. The averaged normalized integrals of product (Int_p) protons and of the starting material (Int_{sm}) protons were used to calculate the reactions' conversion (C,%) using the following formula: $C [\%] = (Int_p / (Int_p + Int_{sm})) \times 100$. When no pure signals of either starting material (7 or a carboxylic acid) could be identified, the signals of DMAP (Int_R) were used instead as mentioned above.

Microscale Reactions Products Screening in the Enzymes Inhibition Assay. After the reaction conversion was determined by semi- q^1 H-NMR, frozen samples of the microscale parallel synthesis were defrosted at room temperature, 50 μ L aliquot was withdrawn from each sample and diluted with the calculated amount of dry DMSO to set the reaction product concentration to 76 μ mol/L. For this, the actual product concentration c_p [mmol/L] in the microscale reaction was calculated using theoretical product concentration (1.25 mmol/L) and the actual reaction conversion rate of each sample C [%] applying the following formula: c_p [mmol/L] = 1.55 mmol/L \times C [%] / 100. Resultant equimolar samples (90 N-acylated acylated 1,2,4-triazol-5-amines) were appropriately diluted to be directly screened at 1 μ M and 100 nM in the enzyme inhibition assays (FXIIa and thrombin) using the fluorogenic substrates. The results of these measurements (triplicate) were expressed as % of inhibition at 1 μ M and 100 nM for each sample.^[37]

Analysis of the Covalent FXIIa-Inhibitor Complex by SEC/ESI-MS. The analysis of covalent FXIIa-inhibitor complex was performed utilizing SEC/ESI-MS as reported previously.^[37] Briefly, 10 μ L of the stock solution (37.67 μ M) of human plasma β -FXIIa (HFXIIAB, >95% purity; Molecular Innovations) were diluted with 90 μ L of purified water. An aliquot of 46.3 μ L was mixed with 3.7 μ L of inhibitor 33 g solution (1 mM in DMSO) to prepare the enzyme-inhibitor solution (molar ratio of 1:20), which was then analyzed via SEC/ESI-MS. Size-exclusion chromatography (SEC) was performed using a MABPac SEC-1 analytical column (150 \times 4 mm, 5 μ m particle size, 300 \AA pore size) from Thermo Fisher Scientific (Bremen, DE). Mass spectrometric detection was carried out using a micrOTOF time-of-flight mass spectrometer from Bruker Daltonics (Bremen, DE) equipped with an electrospray ionization interface. For chromatographic analysis of the sample solutions, isocratic elution was carried out using an aqueous ammonium acetate solution (10 mM, pH 6.8) as mobile phase for 15 min. The enzyme-inhibitor complex was analyzed in the positive ion mode using the following ESI-MS parameters: The mass range was set to m/z 1000–5000, nebulizer gas (nitrogen) was 1.2 bar, dry gas (nitrogen) was 9.0 L/min, dry gas temperature was 200 $^\circ$ C, hexapole RF was 600 V, pre pulse storage time was 30 μ s and transfer time was 100 μ s. Deconvoluted mass spectra were obtained by averaging frames from 6.8 min to 7.6 min retention time and deconvolution using the charge states 9+ to 11+ of the respective protein species.

Acknowledgements

This project was supported by the Deutsche Forschungsgemeinschaft (DFG) grant (DVK: KA 5558/1-1). The authors thank Dr. Jens Köhler and Claudia Thier for recording NMR spectra and Kirstin Lehmkuhl for performing HPLC analysis. Open Access funding enabled and organized by Projekt DEAL.

Conflict of Interest

The authors declare no conflict of interest.

Keywords: FXIIa · thrombin · aminotriazoles · thrombosis · microscale synthesis · parallel synthesis · qNMR · enzyme inhibitors · covalent inhibitors

- [1] D. Ashorobi, M. A. Ameer, R. Fernandez, in *StatPearls*, Treasure Island (FL), 2021.
- [2] J. I. Weitz, J. Harenberg, *Thromb. Haemostasis* **2017**, *117*, 1283.
- [3] a) W. Wienen, J. M. Stassen, H. Pripke, U. J. Ries, N. Huel, *Thromb. Haemostasis* **2007**, *98*, 155; b) L. R. Bush, *Cardiovasc. Drug Rev.* **1991**, *9*, 247; c) M. Sivaraja, N. Pozzi, M. Rienzo, K. Lin, T. P. Shiau, D. M. Clemens, L. Igoudin, P. Zalicki, S. S. Chang, M. A. Estiarte, K. M. Short, D. C. Williams, A. Datta, E. Di Cera, D. B. Kita, *PLoS One* **2018**, *13*, e0201377; d) C. Bouckaert, S. Serra, G. Rondelet, E. Dolusic, J. Wouters, J. M. Dogne, R. Frederick, L. Pochet, *Eur. J. Med. Chem.* **2016**, *110*, 181; e) A. Dementiev, A. Silva, C. Yee, Z. Li, M. T. Flavin, H. Sham, J. R. Partridge, *Blood Adv* **2018**, *2*, 549; f) M. Korff, L. Imberg, J. M. Will, N. Buckreiss, S. A. Kalinina, B. M. Wenzel, G. A. Kastner, C. G. Daniliuc, M. Barth, R. A. Ovsepyan, K. R. Butov, H. U. Humpf, M. Lehr, M. A. Panteleev, A. Poso, U. Karst, T. Steinmetzer, G. Bendas, D. V. Kalinin, *J. Med. Chem.* **2020**, *63*, 13159.
- [4] a) E. Previtali, P. Bucciarelli, S. M. Passamonti, I. Martinelli, *Blood Transfus* **2011**, *9*, 120; b) M. Shoeb, M. C. Fang, *J. Thromb. Thrombolysis* **2013**, *35*, 312; c) N. S. Abraham, P. A. Noseworthy, X. X. Yao, L. R. Sangaralingham, N. D. Shah, *Gastroenterology* **2017**, *152*, 1014.
- [5] a) M. L. Flaherty, *Semin. Neurol.* **2010**, *30*, 565; b) A. Morotti, J. N. Goldstein, *Brain Hemorrhages* **2020**, *1*, 89.
- [6] a) C. Davoine, C. Bouckaert, M. Fillet, L. Pochet, *European Journal of Medicinal Chemistry* **2020**, *208*; b) D. V. Kalinin, *Expert Opin. Ther. Pat.* **2021**.
- [7] T. Renne, E. X. Stavrou, *Front. Immunol.* **2019**, *10*, 2011.
- [8] J. H. Matthews, R. Krishnan, M. J. Costanzo, B. E. Maryanoff, A. Tulinsky, *Biophys. J.* **1996**, *71*, 2830.
- [9] T. D. Goddard, C. C. Huang, E. C. Meng, E. F. Pettersen, G. S. Couch, J. H. Morris, T. E. Ferrin, *Protein Sci.* **2018**, *27*, 14.
- [10] M. Sivaraja, D. M. Clemens, S. Sizikov, S. Dash, C. Xu, M. Rienzo, B. Yang, M. Ryan, M. Chattopadhyay, L. Igoudin, S. S. Chang, S. Keutzer, P. Zalicki, M. A. Estiarte, T. P. Shiau, K. M. Short, D. C. Williams, A. Datta, N. Pozzi, E. Di Cera, C. M. Gibson, K. A. A. Fox, D. B. Kita, *Thromb. Res.* **2020**, *190*, 112.
- [11] E. P. DeLoughery, S. R. Olson, C. Puy, O. J. T. McCarty, J. J. Shatzel, *Semin. Thromb. Hemostasis* **2019**, *45*, 502.
- [12] J. J. F. Chen, D. P. Visco, Jr., *Eur. J. Med. Chem.* **2017**, *140*, 31.
- [13] a) C. L. Allen, A. R. Chhatwal, J. M. Williams, *Chem. Commun. (Camb.)* **2012**, *48*, 666; b) H. Lundberg, F. Tinnis, H. Adolfsson, *Chemistry* **2012**, *18*, 3822; c) X. J. Wang, Q. Yang, F. Liu, Q. D. You, *Synth. Commun.* **2008**, *38*, 1028; d) A. El-Faham, F. Albericio, *Chem. Rev.* **2011**, *111*, 6557; e) C. A. G. N. Montalbetti, V. Falque, *Tetrahedron* **2005**, *61*, 10827; f) E. Valeur, M. Bradley, *Chem. Soc. Rev.* **2009**, *38*, 606; g) S. E. Kim, H. Hahm, S. Kim, W. Jang, B. Jeon, Y. Kim, M. Kim, *Asian J. Org. Chem.* **2016**, *5*, 222.
- [14] P. M. Fischer, *J. Med. Chem.* **2018**, *61*, 3799.
- [15] B. S. P. A. Kumar, B. Madhav, K. H. V. Reddy, Y. V. D. Nageswar, *Tetrahedron Lett.* **2011**, *52*, 2862.
- [16] a) S. S. Tseng, J. W. Epstein, H. J. Brabander, G. Francisco, *J. Heterocycl. Chem.* **1987**, *24*, 837; b) W. M. Eldehna, M. Fares, M. M. Abdel-Aziz, H. A. Abdel-Aziz, *Molecules* **2015**, *20*, 8800.

- [17] a) A. V. Dolzhenko, G. Pastorin, A. V. Dolzhenko, W. K. Chui, *Tetrahedron Lett.* **2009**, *50*, 2124; b) F. P. L. Lim, L. Y. Tan, E. R. T. Tiekink, A. V. Dolzhenko, *RSC Adv.* **2018**, *8*, 22351; c) R. Romagnoli, F. Prencipe, P. Oliva, S. Baraldi, P. G. Baraldi, A. Brancale, S. Ferla, E. Hamel, R. Bortolozzi, G. Viola, *Bioorg. Chem.* **2018**, *80*, 361; d) V. M. Chernyshev, E. V. Tarasova, A. V. Chernysheva, V. A. Taranushich, *Russ. J. Appl. Chem.* **2011**, *84*, 1890.
- [18] P. M. P. Breslow J. L. Selnick H., Egbertson M.; The Rockefeller University. USA. Aminotriazole immunomodulators for treating autoimmune diseases. WO2017123518. 2107.
- [19] a) A. Hijikata-Okunomiya, S. Okamoto, R. Kikumoto, Y. Tamao, K. Ohkubo, T. Tezuka, S. Tonomura, O. Matsumoto, *Thromb. Res.* **1987**, *45*, 451; b) T. Chase, Jr., E. Shaw, *Biochemistry* **1969**, *8*, 2212; c) M. Bohm, J. Sturzebecher, G. Klebe, *J. Med. Chem.* **1999**, *42*, 458.
- [20] A. E. Harms, *Org. Process Res. Dev.* **2004**, *8*, 666.
- [21] G. M. Sheldrick, *Acta Crystallogr A Found Adv* **2015**, *71*, 3.
- [22] G. M. Sheldrick, *Acta Crystallogr C Struct Chem* **2015**, *71*, 3.

Manuscript received: June 15, 2021
Accepted manuscript online: July 18, 2021
Version of record online: August 4, 2021